UNIVERSIDADE DE LISBOA
FACULDADE DE CIÊNCIAS
DEPARTAMENTO BIOLOGIA VEGETAL

Understanding the mechanisms at the onset of LAMA2-congenital muscular dystrophy

Cláudia Sofia Paulino Cavaco

Mestrado em Biologia Molecular e Genética

Dissertação orientada por:
Prof. Dra. Sólveig Thorsteinsdóttir
Prof. Dra. Ana Rita Carlos

2023

Acknowledgments

This was a difficult and challenging year that tested all my abilities.

First, I want to start by thanking to the most important person in my life, my son Martim. I am very gratefully for him to be on boarded this great adventure that ended up having some impact on our routine. I hope that one day he will be very proud of all my achievements. Of course, this merit in my life would not have been possible without the help, support and motivation of my husband Luis Cavaco which also deserves a huge thank you. A special thank to my parents for all effort and support in this difficult year.

This experience and learning would not have been possible without my two supervisors, Ana Rita Carlos and Sólveig Thorsteinsdóttir. I want to thank Rita for guiding me and always being present in moments of despair, from which she always calmly found a solution. And, of course, the greatest motivator of our walks. To Sólveig for always be available and encouraging each challenge in this project.

Special thanks to my mentor Susana Martins who was always present to guide and help me when I couldn't be there due to my job. My partner in weekly laboratory tasks and a great great teacher.

My master partner's, Diogo Fernandes, Maria Neves and Andreia Conceição for all the shares and concerns throughout our projects and to all the fun moments we had. Individually to Diogo "chefinho" for sharing with me the knowledge regarding bacterial cloning and CRISPR/Cas9. To "baby" Maria and Andreia "contra factos não há argumentos" for taking care of my membranes.

I also want to thank Vanessa Ribeiro, our public relations, for the motivation and availability to help whenever needed and to Pedro Santos "o rei" for joining in our jokes. I also want to thank the rest of the DEM group, Ana Lopes, Gabriela Rodrigues, Rita Zilhão, Luís Marques and António Cordero for sharing their knowledge. I also want to highlight the unity and commitment of the DEM group at the competitions in which we won the cup at cE3c events.

Last but not least, I want to thank to Marta Palma for all the lab support.

Abstract

LAMA2-congenital muscular dystrophy (LAMA2-CMD) is characterized by muscle weakness and hypotonia present at birth and, currently, no treatment or cure are available. LAMA2-CMD is linked to mutations in *LAMA2*, which encodes the laminin α2-chain, a component of laminin 211 (LN211), which is the most important laminin isoform in mature skeletal muscle. Using the dy^W/dy^W mouse model for LAMA2-CMD, the host laboratory and collaborators established that the disease onset occurs during fetal development, with muscle growth impairment, numerical reduction of muscle stem cells and myoblasts, and overactivation of the JAK-STAT3 signaling pathway. Our latest results also point to a role of the focal adhesion kinase (FAK) in this process. To understand which mechanisms trigger these defects, a *Lama2*-deficient C2C12 myoblast cell line was established. Preliminary studies with *Lama2*-deficient cells showed alterations in proliferation and differentiation, as well as an increase in DNA damage and oxidative stress. The aim of this project was to test whether inhibition of FAK and/or STAT3 counters the LAMA2-CMD phenotype *in vitro*. For that, first the cell lines required were generated and their differentiation was analyzed. Data confirmed the impaired differentiation of *Lama2*-deficient cells and revealed a significant increase of both nuclear and cytoplasmic NFIX, while MYF5 is apparently retained in cytoplasm in *Lama2*-deficient cells, both key factors in myogenesis. Subsequently, these cell lines were used to titrate the FAK and STAT3 inhibitor concentrations and to test the efficiency of shRNA targeting FAK and STAT3. Results indicate that the use of FAK inhibitor (3 µM for 2 hours) tends to reduce STAT3 levels, while a reduction in oxidative stress was not observed. All findings together, will certainly contribute towards a better understanding of the mechanisms underlying the first steps of LAMA2-CMD, which is essential for the development of therapies targeting the primary events of this incurable disease.

Keywords: *Lama2*, LAMA2-CMD, STAT3, FAK, differentiation.

Resumo

A distrofia muscular congénita LAMA2 (LAMA2-CMD) é uma doença hereditária autossómica recessiva caracterizada pela manifestação de sintomas como fraqueza muscular grave e hipotonia. O diagnóstico desta doença neurodegenerativa é feito à nascença ou nos primeiros meses de vida, as manifestações da doença vão agravando cada vez mais com o passar do tempo e, como consequência, a esperança média de vida dos afetados é reduzida. Atualmente, esta doença afeta cerca de 1 a 4 em cada 100.000 pessoas em todo o mundo, muitas das quais são crianças. Até à data, os tratamentos disponíveis são direcionados para o melhoramento e alívio dos sintomas, não existindo ainda tratamento ou cura eficaz. Mutações no gene *LAMA2* são a principal causa da LAMA2-CMD. Este gene codifica a cadeia α2 das lamininas, presente na glicoproteína laminina-211 (LN211) e também na laminina-221 (LN221). A LN211 é a isoforma mais importante presente no músculo esquelético maduro e desta forma o impacto ao nível do músculo esquelético é tremendo na presença de mutações em *LAMA2*. Ao nível celular, as lamininas encontram-se numa rede de componentes não celulares presentes em todos os tecidos, sendo conhecida como matriz extracelular (ECM). A ECM fornece suporte físico às células e é composta, entre outros componentes, por colagénios, fibronectina e lamininas. A ECM é também responsável pela sinalização extra e intracelular através de fatores de crescimento e moléculas bioativas que controlam o crescimento celular através da proliferação, migração, diferenciação e até apoptose. Desta forma, mutações em componentes da ECM são a principal causa de muitas distrofias musculares. As lamininas quando se ligam aos recetores membranares integrinas desencadeiam uma série de sinais responsáveis pela adesão, diferenciação e migração celular na fase embrionária do desenvolvimento muscular.

Através do uso de um modelo animal de ratinho para LAMA2-CMD, dy^W/dy^W (*dyW*), o laboratório, juntamente com os seus colaboradores, estabeleceu que os primeiros sintomas da doença ocorrem entre o dia embrionário 17.5 (E17.5) e o dia E18.5, com comprometimento do crescimento muscular e redução no número de células estaminais musculares (MuSCs) e mioblastos. Ao estudar o músculo esquelético fetal de ratinhos *dyW*, foi observado que vias de sinalização como o caso das vias JAK/STAT3 e, mais recentemente, da cinase de adesão focal (FAK), se encontram com atividade superior ao normal na ausência da proteína laminina-α2 funcional em comparação com os ratinhos selvagem. Para estudar e perceber em detalhe quais os mecanismos que desencadeiam o aparecimento desta doença, foi gerada uma linha celular de mioblastos C2C12 mutado no gene *Lama2* através da técnica de edição de genes CRISPR/Cas9. Para além da reduzida expressão no gene *Lama2*, estas células são caracterizadas por apresentarem alterações de proliferação, diferenciação, bem como o aumento de danos no DNA e stress oxidativo.

A relação entre as vias FAK e JAK/STAT3 ainda não é conhecida bem como a sua influência direta na proliferação e diferenciação celular na ausência de laminina-α2 funcional. O que se sabe é que a ativação destas vias está dependente, entre outras, da sinalização através das lamininas. Na presença de mutações nas lamininas, a sua ligação às integrinas fica comprometida bem como a sua transmissão de sinal. Sendo que as vias do FAK e JAK/STAT são vias que estão relacionadas com a proliferação e diferenciação das células, pensa-se que na ausência da sinalização das lamininas, as células induzam o aumento de expressão de algumas vias. O problema associado é que a ativação excessiva pode ser prejudicial para as células e não se verifique o efeito pretendido pelas mesmas. Resultados anteriores obtidos pelo laboratório mostraram também alterações em alguns fatores de transcrição (TF) envolvidos na miogénese. Estes fatores são responsáveis pela ativação de expressão génica coordenada que induz o momento exato em que as células musculares devem proliferar ou diferenciar. A proteína associada ao sim (YAP), o fator nuclear 1 tipo X (NFIX) e o fator miogénico 5 (MYF5) são alguns TF com alterações na ausência de *Lama2*. A proteína YAP, como o próprio nome indica, é uma proteína que necessita da associação de outros elementos para desempenhar a sua função no núcleo ou ser degradada por fosforilação no citoplasma quando a sua atividade não é necessária. A atividade do YAP está

associada a proliferação celular enquanto que na diferenciação celular o YAP é sinalizado por fosforilação para degradação no citoplasma. Desta forma o YAP pode ser indicado como marcador de proliferação celular. A atividade do YAP pode também estar relacionada com a atividade do MYF5 na proliferação celular, uma vez que o domínio ativador de intensificação de transcrição (TEAD), parceiro de ligação do YAP, é também um elemento necessário para ativação do MYF5. O MYF5 é um dos primeiros fatores miogénicos a ser transcrito no desenvolvimento muscular enquanto que o NFIX é responsável pela transição entre os estádios embrionário e fetal. Recentemente, o papel do NFIX foi também associado à regulação do stress oxidativo causado por danos no musculo esquelético.

Tendo em conta o papel crucial da diferenciação no desenvolvimento do músculo, este projeto pretende pesquisar *in vitro* o efeito fenotípico da LAMA2-CMD através da inibição do FAK e/ou STAT3. Para tal, a linha celular mutada no gene *Lama2* foi gerada através da técnica de edição de genes CRISPR/Cas9. A caracterização desta linha celular foi confirmada tendo em conta o fenótipo previamente conhecido, como a baixa expressão do gene *Lama2*, stress oxidativo causado por danos no DNA e a ativação aumentada do STAT3. Genotipicamente foi também confirmado que esta linha celular apresenta alterações nucleotídicas na zona de corte. A análise de diferenciação celular confirmou a existência de defeitos na formação de miofibras em células com ausência de *Lama2*. Centrando as atenções em alguns fatores miogénicos, os dados também confirmaram o aumento nuclear e citoplasmático do NFIX, enquanto que o MYF5 está aparentemente retido no citoplasma. De acordo com a alterações verificadas nas vias de sinalização do FAK e STAT3, foram posteriormente utilizados inibidores farmacológicos para perceber os efeitos fenotípicos causados pela inibição dos mesmos. Após o estabelecimento da concentração ideal do inibidor do FAK (3 µM durante 2 horas) os resultados demonstraram uma tendência na redução dos níveis de P-STAT3. Contrariamente, o mesmo não foi observado com a diminuição do stress oxidativo nem dos níveis de NFIX. Adicionalmente foi também testado se as células tratadas com inibidor do FAK conseguiam reverter os efeitos associados com a formação de miofibras, mas os resultados obtidos não revelaram alterações. Para avaliar os efeitos a longo prazo da inibição das proteínas FAK, STAT3 e NFIX foi aplicada uma abordagem genética de silenciamento de RNA. Apesar da confirmação, por sequenciação de Sanger, que as sequências alvo estavam corretamente inseridas no plasmídeo, os resultados obtidos não revelaram redução na expressão das mesmas. Novos ensaios necessitam de ser feitos, tendo em consideração um novo plasmídeo, pois pensa-se que o problema esteja associado à durabilidade de armazenamento do plasmídeo usado.

Em suma, a inibição da proteína FAK revelou que a via de sinalização do FAK está de alguma forma diretamente relacionada com a via JAK/STAT3. Os tratamentos a curto prazo não são suficientes para reverter o efeito do stress oxidativo associado às células mutadas em *Lama2* e consequencialmente não são verificadas alterações nos níveis de NFIX bem como diferenças na formação de miofibras. Os tratamentos de inibição com efeito a longo prazo podem ser a chave para a redução do stress oxidativo e formação correta de miofibras em células mutadas para *Lama2*.

Desta forma, todos os resultados em conjunto contribuirão certamente para uma melhor compreensão dos mecanismos subjacentes aos primeiros indícios da LAMA2-CMD, o que é essencial para o desenvolvimento de terapias que visem especificamente os eventos primários desta doença incurável.

Palavras-Chave: *Lama2*, LAMA2-CMD, STAT3, FAK, diferenciação.

Index

List of Figures

List of Tables

List of abbreviations and symbols

Arbp0/Rplp0 – Acidic ribosomal phosphoprotein P0/ Large ribosomal protein
BSA – Bovin serum albumin
cDNA – Complementary DNA
CMD – Congenital muscular dystrophy
CRISPR/Cas9 – Cluster regularly interspaced short palindromic repeats associated protein 9
Ct – Threshold cycle
DAPI – 4`,6-diamidino-2-phenylindole
DMD – Duchene muscular dystrophy
DMEM – Dulbecco´s modified eagle´s medium
DMSO – Dimethyl sulfoxide
DTT – Dithiothreitol
E17.5 – Embryonic day 17.5
E18.5 – Embryonic day 18.5
ECM – Extracellular matrix
Eno3 – β-enolase
FACS – Fluorescence activated cell sorting
FAKi – FAK inhibitor
FAK – Focal adhesion kinase
FAT – Focal adhesion targeting
FBS – Fetal bovine serum
FERM – 4.1 protein, ezrin, radixin, moesin
Fwd – Forward
GAPDH – Glyceraldehyde-3-phosphate dehydrogenase
GFP – Green fluorescent protein
GOI – Gene of interest
gRNA – Guide RNA
HBS – HEPES buffered saline
HEK 293T – Human embryonic kidney cells
HEPES - 4-(2-hydroxyethyl)-1-piperazineethanesulfonic acid
HO-1 – Heme-oxygenase 1
HRP – Horseradish peroxidase
IL6 – Interleukin 6
JAK/STAT – Janus kinase signal transducer and activator of transcription
KO – Knockout
LAMA2-CMD – Laminin- α2 congenital muscular dystrophy
***Lama2* KO** – Lama2 knockout C2C12 cells
LATS1/2 – Large tumor suppressor ½
LB – Lysogeny broth
LG – Laminin G-like domain
LN – Laminin N- terminal domain
MBD2 – Methyl CpG-binding protein 2
MCK – Muscle creatine kinase
MDC1A – Merosin -deficient congenital muscular dystrophy type 1A
MEF2 – Myocyte enhancer factor 2
MRFs – Myogenic regulator factors
MRF4 – Myogenic regulator factor 4
mRNA – Messenger RNA
MuSC – Muscle stem cell
Myf5 – Myogenic factor 5
Myl1- Myosin light chain 1
MyoD – Myogenic differentiation
Myog – Myogenin
NEB – New england biolabs
NES – Nuclear export sequence
NFIX – Nuclear factor 1X
NLS – Nuclear localization sequence
PAM – Protospacer adjacent motif
PBS – Phosphate-buffered saline
P-FAK – Phosphorylated FAK
P-FAK Y397 – FAK phosphorylated on tyrosine 397
PNK – Polynucleotide kinase
P-STAT3 – Phosphorylated STAT3
P-STAT3 Y705 – STAT3 phosphorylated on tyrosine 705
PVDF – Polyvinylidene fluoride
Rev – Reverse
ROS – Reactive oxygen species
RT – Room temperature
SDS-PAGE- Sodium dodecyl sulfate – polyacrylamide gel electrophoresis
Ser127 – Serine 127
shRNA – Short hairpin RNA
STAT3 – Signal transducer and activator of transcription
STAT3i – STAT3 inhibitor
TAZ – WW domain containing protein 1
TBST – Tris buffered saline 0,1% tween
TEAD1-4 – Transcriptional enhancer factor domain 1-4
TF – Transcription factors
TRC – The RNAi Consortium
Tubb6 – Tubulin beta 6 class V
Tyr397 – Tyrosine 397

Ubc9 – Ubiquitin conjugated enzyme 9
YAP – Yes-associated protein
WB – Western blot
WT – Wildtype

1. Introduction

1.1. Laminins and extracellular matrix-cell communication

The extracellular matrix (ECM) is the non-cellular component of tissues that provides physical support for cells and allows the crosstalk between the intra and extracellular environment. The correct development of organisms requires the organization of ECM multidomain macromolecules in a structurally stable complex, which is responsible for the maintenance of cell and tissue homeostasis, as well as the control of cellular processes of vital importance such as proliferation, adhesion, migration, polarity, differentiation, and apoptosis [1,2]. The ECM is highly dynamic and has the capacity to respond to some environmental stimuli, such as applied force or injury, both of which are important for development and disease. For this reason, the ECM is in constant remodeling [3] and is constituted by approximately three hundred proteins with distinct physical and biochemical properties, collectively termed matrisome, which include laminins, collagens, and fibronectin (**Figure 1.1A**) [2].

Laminins are heterotrimeric glycoproteins (400-800 kDa) mainly present in basement membranes, a type of ECM, and are expressed in several tissues including skeletal muscle. Laminins are composed of α-, β- and γ -subunits bound as a cross-shaped molecule (**Figure 1.1B**). The subunits assemble into at least sixteen known different laminin heterotrimers to form networks that remain in close association with cells through interactions with cell surface receptors [2,4,5]. Laminins are essential for initial embryonic development and organogenesis, allowing the correct communication between the intracellular and extracellular environment, via direct binding to different transmembrane receptors, such as integrins. Integrins are heterodimeric transmembrane proteins and bidirectional signaling receptors responsible for communication with the ECM and cell cytoskeleton. In the extracellular side, they are activated by matrix ligands leading to conformational changes that allow, among other features, the binding of focal adhesion kinase (FAK) [2,6,7]. In skeletal muscle laminin-211 and laminin-221 (α2, β1 and γ1 chains) are the most abundant isoforms in healthy adult [8,9]. Integrin-α7β1 plays a crucial role during embryonic development and regeneration in adult skeletal muscle by facilitating myoblast adhesion to laminin-211, -221, as well as to laminin-111 [9]. In addition to the FAK signaling pathway, the binding of laminins to integrin receptors on the cell surface promotes the activation of several others pathways, including Janus kinase (JAK)/signal transducer and activator of transcription (STAT) pathway leading to cell proliferation, cell differentiation and cell survival [10]. Considering the key role of laminins in ECM-cell communication, it is not surprising that they are essential for proper embryonic development and that mutations in laminins lead to different pathologies.

A.

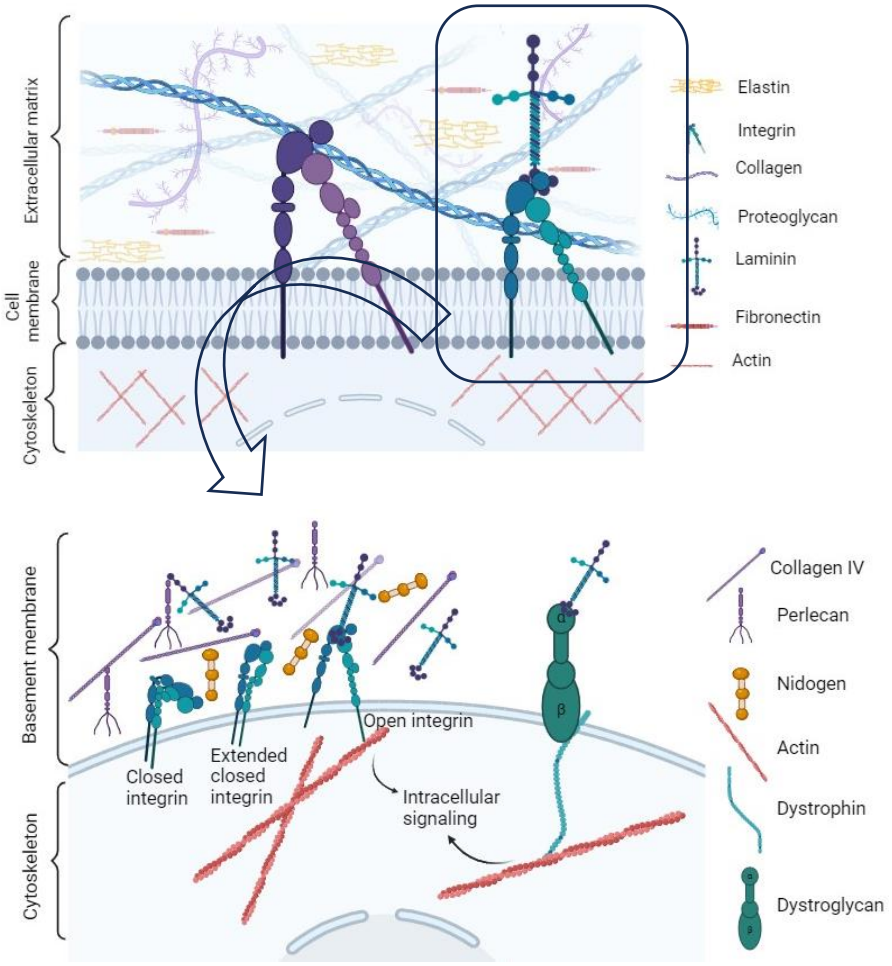

B.

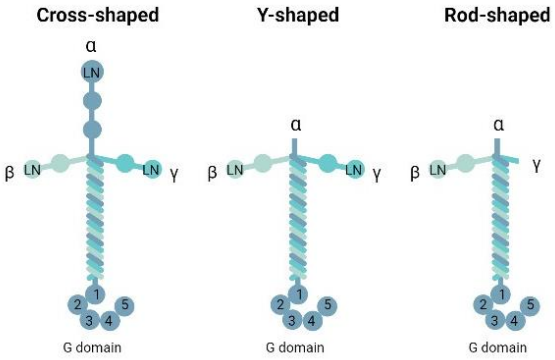

Figure 1.1 – Extracellular matrix structure and intracellular communication. A. Schematic representation of extracellular matrix (ECM), cell membrane and cytoskeleton. The ECM is composed of two main classes of macromolecules, the proteoglycans, and the fibrous proteins – collagens, elastins, fibronectins and laminins. The ECM that is in close contact with the cells providing a scaffold is called basement membrane (zoomed below), and is mainly composed of perlecan, nidogen, collagen IV and laminins. In skeletal muscle, the laminins and collagen IV interact with open integrins, which connect to actin through intermediate proteins e.g. talin and α-actin. Laminins also interact with actin via linkage with dystroglycan complex and dystrophin. **B.** Schematic image of heterotrimeric laminins showing the three main laminin shapes determined by the combinations of the α, β, and γ subunits: Cross-shaped, y-shaped, and rod-shaped. The three chains trimerize to form the long arm in a coiled-coil manner, with a C-terminal laminin globular domain (LG) that consists of five smaller units (LG1-5). The short arms include the laminin N-terminal domain (LN). Images created in BioRender.com.

1.2. Myogenesis - the development of muscle

The human body is a composite of multiple types of tissues, for example muscle. The muscle is subdivided into three structural types: cardiac muscle, smooth muscle, and skeletal muscle [11]. Skeletal muscle is the organ responsible for specific movements via its intrinsic excitation-contraction and connection processes. It is essential for maintaining posture and balance, respiration, and protection of the vital organs in the body [12].

Myogenesis is the process of skeletal muscle development and can be divided into three phases: 1) Embryonic myogenesis; 2) Fetal myogenesis; 3) the myogenic phase that occur after birth [13].

The first steps in skeletal muscle formation are commanded through expression of the paired domain homeobox PAX transcription factors (TF) (Pax3 and Pax7). Pax3 is mainly expressed during early skeletal muscle formation and is detected during somite formation (somitogenesis), while Pax7 is more expressed during fetal development, post-natal growth and adult muscle regeneration [13,14].

During embryonic myogenesis, the paraxial mesoderm that is derived from the primitive germ layers in the embryo is responsible for the skeletal muscle formation in the trunk and limbs. The head muscles are derived from paraxial head mesoderm and from the prechordal mesoderm [13]. Paraxial mesoderm segments into pairs of epithelial somites, the first metameric structure in mammalian embryos. Depending on their spatiotemporal orientation, the mature somites receive signals from adjacent tissues and undergo differentiation. In a ventral position, the somites give rise to the mesenchymal sclerotome, which is committed to generate precursors for cartilage and bone, while in the dorsal position, the somites remain epithelial known as the dermomyotome. Posteriorly, the dermomyotome gives rise to muscle stem cells (MuSCs), the precursors of the skeletal muscle lineage. MuSCs start differentiating into myoblast and later into muscle fibers (**Figure 1.2**), which is regulated by myogenic regulatory factors (MRFs) [13–15]. The MRFs are key players in prenatal skeletal muscle formation, postnatal skeletal muscle growth and muscle regeneration. The MRFs include Myogenic Factor 5 (Myf5), Myogenic Differentiation (MyoD), Myogenin (Myog) and Myogenic Regulatory Factor 4 (MRF4) [16]. Myf5 is the first MRF to be expressed in the mouse embryo and is responsible for directing the cells into the skeletal muscle program and its expression is also maintained in quiescent satellite cells [17]. During somitogenesis, the tissues surrounding somites play a key role in sending signals that direct myogenesis.

According to the spatiotemporal position, the expression of *Myf5* is regulated by different enhancers present in a well characterized locus in mouse chromosome 10 [17,18]. In the same chromosome upstream of *Myf5* gene, the *MRF4* gene and some *Myf5* enhancers interact with *MRF4* expression in equilibrium based on their spatiotemporal position [17,18]. *MyoD* expression is maintained in the proliferative phase until the initial differentiation phase, when *Myogenin* is expressed and the cell cycle exit is triggered, the differentiation, and fusion of myoblasts that form multinucleated myofibers occurs [16]. Myf5 allows the activation of muscle progenitor cells which transit to myoblasts (muscle precursor cells) [13]. In subsequent steps, the myoblasts start expressing MyoD and Myogenin, which allow their differentiation into myotubes (muscle cells). Therefore, in quiescent cells, MyoD and Myogenin are commonly used as myogenesis markers for activation and differentiation, respectively [19]. During embryogenesis, fetal and postnatal growth, the myoblasts then fuse into multinucleated muscle fibers (myofibers) induced by the expression of MRF4 [20].

Myofibers, the terminally differentiated post-mitotic cells, are composed of overlapping thick and thin filaments (myofilaments) that are arranged longitudinally into sarcomeres, which cause the striated appearance of skeletal muscle [11,21]. The mature myofibers are supplied with nutrients and oxygen by blood vessels and are innervated by a single motor neuron via the neuromuscular junctions [13].

Adult skeletal muscle has the capacity to regenerate after muscle injury, among other traumas. This self-renewal ensures tissue homeostasis and occurs through the activation of satellite cells (quiescent MuSCs), which are located between the sarcolemma and the basement membrane of muscle fibers. The

satellite cells exit the quiescent state and have the capacity to proliferate and differentiate, thereby generating new fibers or repairing damaged fibers [15,19].

Together, these myogenic regulatory factors have a tight regulation of expression in a sequential manner which regulate other factors [19] involved in myogenesis and maintenance of skeletal muscle. Some of these players will be described below.

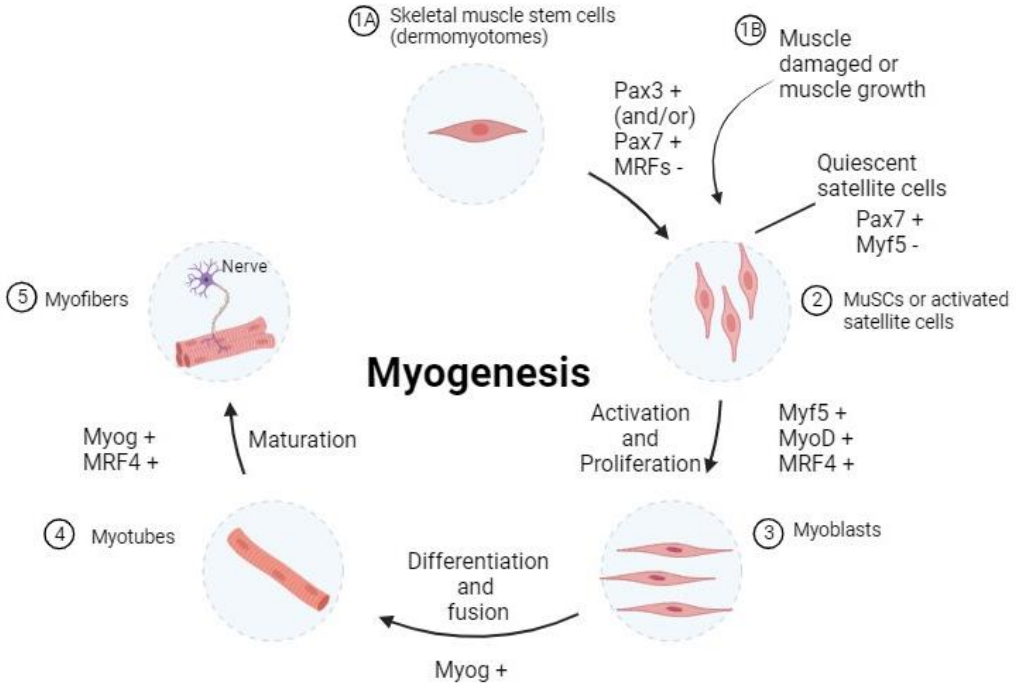

Figure 1.2 - Myogenesis and its regulation. Schematic representation of skeletal muscle development commanded by the expression of myogenic regulatory factors (MRFs) during the different stages of development. (**1A**) Expression of the transcription factors Pax3 and/or Pax7 marks the embryonic muscle progenitors in the dermomyotome and myotome as muscle stem cells (MuSCs). (**2**) The expression of MRFs is induced by variety of external stimuli. The expression of Myf5, MyoD and/or MRF4 commit MuSCs to become myoblasts which are capable of proliferating. (**3**) Soon after, myoblasts start expressing Myogenin and exit the cell cycle. (**4**) MRF4 is expressed during maturation state, when myofibers (**5**) begin to be vascularized and innervated. In adult skeletal muscle, some satellite cells remain in a quiescent state just with the expression of Pax7. This reserve of MuSCs is important in situations of muscle growth and repair after damage (**1B-5**) where Myf5 becomes expressed in these cells and the whole myogenesis process is repeated leading to the formation of new myofibers and/or the repair of damaged fibers. Image created in BioRender.com.

1.2.1 NFIX during muscle development

NFIX (nuclear factor 1X) is a transcriptional factor member of the *Nfi* gene family (*Nfia*, *Nfib*, *Nfic*, and *Nfix*) that act as transcriptional activators or repressors of cellular and viral genes [22,23]. The *Nfix* gene is the only member of the *Nfi* gene family that is expressed during skeletal muscle development, specifically in fetal myoblasts but not in embryonic myoblasts [23]. Therefore, *Nfix* acts as a regulator of the transcriptional switch between embryonic and fetal myogenesis. The expression of *Nfix* in fetal muscle is coincident with Pax7 which binds to the *Nfix* promoter. *Nfix* activates the expression of fetal muscle-specific genes, such as muscle creatine kinase (MCK) and β-enolase (Eno3), that inhibit the transcription of embryonic muscle-specific genes, such as slow myosin heavy chain [22,24]. Recently, NFIX was found to be crucial to the maintenance of skeletal muscle regeneration upon injury [23]. In normal conditions, *Nfix* expression is also crucial to the induction of controlled regeneration in injured muscle while protecting from oxidative stress caused by damaged fibers. Thus, NFIX may play a role

in regulating oxidative stress in muscles. However, overexpression of *Nfix* in muscular dystrophies is associated with increased cycles of regeneration and degeneration that intensify the pathology. Increased oxidative stress under such conditions is associated with oxidative stress induced by damage and degeneration [24,25]. A recent study using a dystrophic *Nfix* null mouse model revealed a protective effect of deleting *Nfix* against the progression of the pathology, even when the signals of the disease are already present [25].

1.2.2 FAK and STAT3 signaling in muscle development

In addition to the role of transcription factors during myogenesis, there are extracellular signals that induces the activation of some signaling pathways that regulate cell proliferation and differentiation.

Due to its direct interaction with integrins, FAK is one of the key pathways activated in response to mechanical force or clustering in adherent cells [26,27]. It may also be activated by growth factors and cytokines signalings [28]. FAK is a member of the cytoplasmic non-receptor protein-tyrosine kinase family and can promote cell adhesion, migration, and proliferation in different types of cells [29]. It is a multidomain protein composed of three major domains: The N-terminal containing the FERM (Four-point-one, Ezrin, Radixin, Moesin) domain, Central kinase domain, and the C-terminal with the FAT (focal adhesion targeting) domain [27,28,30]. The FERM domain, is the main regulatory domain of FAK activity and is critical for the interaction and activation of other proteins. The FERM domain binds directly to the kinase domain C-lobe when FAK is auto-inhibited by a loop that protects FAK from activation [31] (**Figure 1.3A**). In response to extracellular stimuli, the FERM domain is released from the intramolecular interaction and the activation loop is exposed to Tyr397 (tyrosine 397) autophosphorylation. Phosphorylation on Tyr397 creates a high affinity binding site for Src non-receptor tyrosine kinase and Src family kinase to a full catalytic activation [27,29–31].

As previously mentioned, muscle development is regulated by MRFs. FAK activity is one of the important cell cycle regulators of myoblast proliferation via the induction of MyoD expression. When myoblasts undergo differentiation, FAK activity is reduced until myoblast differentiation is complete, while myoblast fusion promoted when the activity of FAK is restored. The reduction in FAK activity between stages is critical for correct myogenesis. In muscular dystrophies the activation of satellite cells and increased myoblast differentiation is an attempt to restore muscle via FAK activation [28].

Moreover, FAK can shuttle between the cytoplasm and the nucleus due to nuclear export signals (NES) in its kinase domain, as well as nuclear localization signals (NLS) in the FERM domain. The oxidative stress can promote FAK nuclear localization as a coreceptor of TF and, for instance, induce myoblast differentiation through its interaction with MBD2 (methyl CpG-binding protein 2) by chromatin remodeling [32,33] (**Figure 1.3B**).

Apart from FAK signaling, another pathway important for intracellular and extracellular communication in muscle development, is the JAK/STAT pathway. STAT3 is a cytoplasmatic TF activated by interleukin 6 (IL6)/JAK/STAT3 signaling pathway and plays an essential role in cell proliferation, migration and apoptosis [34]. In normal conditions, all cells exhibit low expression of STAT3, while its activation is dependent on several external stimuli from the ECM [35]. IL6 is expressed by local tissue inflammation and the tyrosine kinase receptors in the plasma membrane, which induces activation of downstream signaling molecules, such as JAK/STAT pathway [36]. The activation of STAT3 is required for quiescent MuSC activation in response to muscle injuries, but recent studies show that it is also involved in myogenesis and the regeneration process [35]. The phosphorylation on tyrosine 705 activates STAT3 (P-STAT3) and induces its translocation to the nucleus where it regulates expression of genes such as *Myod*, myocyte enhancer factor 2 (*Mef2*), and *Myog* [34,37] (**Figure 1.3B**). The JAK/STAT3 pathway is required for efficient muscle fiber adaptation and for that different JAK/STAT combinations lead to distinct cellular responses linked to muscle proliferation and differentiation. The

JAK1/STAT1/STAT3 combination promotes myoblast proliferation through *MyoD* and *Mef2* expression and prevents the premature differentiation into myotubes, while the JAK2/STAT2/STAT3 combination induces myogenic differentiation [37,38]. Due to the role of STAT3 in satellite cell function, STAT3 is activated to promote differentiation, generate new fibers, or induce myoblasts to fuse with existing myofibers in response to muscular dystrophies [37,39]. Hight levels of P-STAT3 have been described to be beneficial in diseases such as congenital myotonic dystrophy type 1 (CDM) and Duchene muscular dystrophy (DMD), because they ameliorate the disease phenotype. However, persistently high levels of P-STAT3 can also lead to muscle wasting, hence becoming detrimental in these muscular dystrophies [37].

The link between these two signaling pathways was demonstrated through Src protein, that is involved in signal transduction of the cell surface receptors mediated by integrin/FAK to upregulate their downstream signaling targets such as the JAK/STAT3 pathway [40,41]. It was also reported that Src regulate the yes-associated protein (YAP), a transcriptional co-regulator activated downstream of FAK and STAT3 pathways [40,42]. The mechanical signals involved in YAP activation are transduced into cell-specific transcriptional responses to allow the regulation of cell proliferation, differentiation, survival, organ growth and stem cell self-renewal [43,44]. Src affects YAP activation through three main mechanisms: (1) Direct phosphorylation through tyrosine; (2) activation of pathways repressing Hippo kinases; and (3) Hippo-independent mechanisms [40]. The Hippo pathway is the main YAP activity regulator through negative feedback, meaning that Hippo pathway activation leads to YAP inactivation. Many upstream signals, such as cell polarity, mechanical cues, cell density, metabolic challenges, and stress signals, are able to modulate the Hippo pathway [45,46]. When the Hippo pathway is activated, serine 127 (ser127) YAP is phosphorylated by LATS1/2 kinase leading to the retention and degradation of YAP in the cytoplasm. This mechanism promotes skeletal muscle differentiation through cell density, in monolayer culture [44,45]. On other hand, when the Hippo pathway is inactive (e.g Src signaling), the YAP and its homolog TAZ (WW domain containing protein 1) translocate into the nucleus to interact with transcriptional enhancer factor domain 1-4 (TEAD1-4) to promote cell proliferation via transcription of its target genes. In striated muscle, YAP acts as a positive regulator of cell size and in abnormal conditions YAP inactivation can lead to muscle fibers atrophy [45,47].

A.

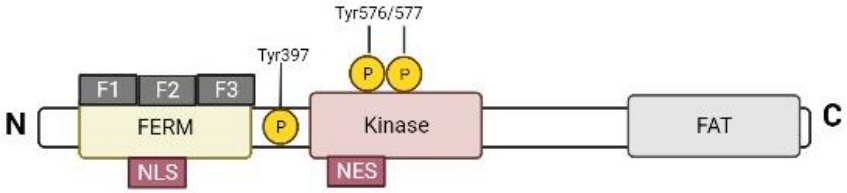

B.

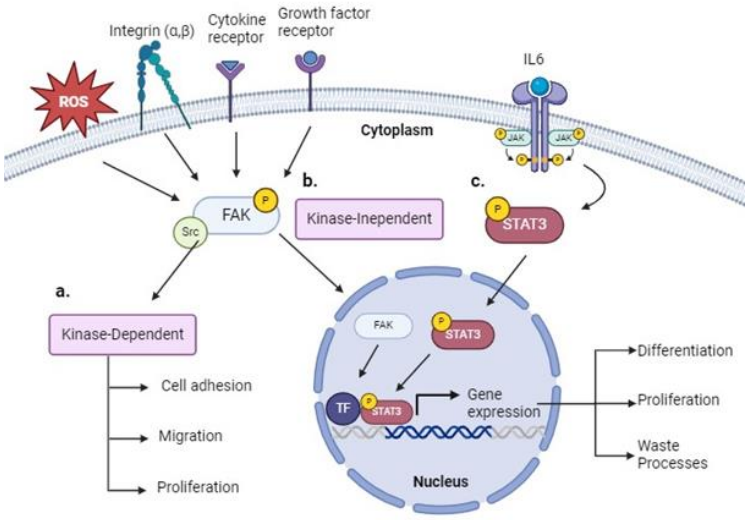

Figure 1.3 - FAK and JAK/STAT3 pathways activation in skeletal muscle development. A. Representative molecular structure of domains and important FAK phosphorylation sites. The three main domains of FAK are the FERM (Four-point-one, ezrin, radixin, moesin), the central kinase and the FAT (focal adhesion targeting) domains. The FERM domain is divided into three subunits (F1, F2 and F3) and contains a nuclear localization sequence (NLS), while the nuclear export sequence (NES) is localized in the kinase domain. Tyrosine 397 (Tyr397) autophosphorylation enables a strong binding affinity for Src kinase family and the phosphorylation of Tyr576 and Tyr577 results in full FAK activation. N-terminal and C-terminal are represented with N and C respectively. **B.** Schematic representations of FAK and JAK/STAT3 pathways and their role in skeletal muscle development. (**a**) Integrins, cytokines receptors and growth factor receptors induce FAK kinase-dependent activation through Src binding leading to cell adhesion, migration, and proliferation of muscle cells. (**b**) FAK kinase-independent activation is induced by oxidative stress (due to increased levels of reactive oxygen species, ROS), active FAK translocates to the nucleus and induces myoblast differentiation by interaction with transcription factors (TF), including MBD2 (methyl CpG-binding protein 2) (**c**) The JAK/STAT3 pathway can be activated through interleukin 6 (IL6) signaling. Phosphorylated STAT3 induced by phosphorylated JAK, translocates to the nucleus to regulate the expression of genes involved in myoblast proliferation, differentiation, and muscle waste processes, including *Myod*, myocyte enhancer factor 2 (*Mef2*), and *Myog*. Images created in BioRender.com.

1.3. Laminin-α2-related congenital muscular dystrophy (LAMA2-CMD)

Extracellular signals, as previously mentioned, trigger input cascades through the activation of numerous signaling pathways. The stability of the ECM provides the correct signal reception by integrins and downstream signaling pathways that transmit this signal to the cytoskeleton. Therefore, mutations linked to ECM signaling are associated with multiple diseases, for example congenital muscular dystrophies (CMDs).

CMDs are clinically and genetically a group of neuromuscular disorders that includes the Laminin-α2-related congenital muscular dystrophy (LAMA2-CMD), previously called merosin-deficient congenital muscular dystrophy type 1A (MDC1A). LAMA2-CMD is a genetic disease caused by mutations in the *LAMA2* gene, which encodes the laminin-α2 chain of laminins 211 and 221. LAMA2-CMD is inherited in autosomal recessive manner and is usually diagnosed at birth or in early childhood. This disease is the most common CMD in the world affecting around 1 to 4 in every 100,000 people and represent around 30-50% of total CMD diagnosed in Europe [8–10,48]. As mentioned before, laminins are important ECM molecules present in basement membrane where they interact directly with integrins and dystroglycans [2]. Mutations in the *LAMA2* gene are loss-of-function mutations that may be, for example, missense mutations, in-frame deletions, or splice site mutations. These mutations may lead to a complete absence of, or a partial deficiency in, the laminin-α2 chain. Depending on the type of mutation, the disease severity can range from highly severe early-onset to a mild late-onset muscular

dystrophy [9,10,49]. The main symptoms of LAMA2-CMD are muscle weakness, delayed motor development, joint contractures, respiratory failure, defects in peripheral and central nervous system, and brain structural defects [10,50]. During muscle development the disruption of the basement membrane impacts the downstream signaling pathways. This leads to higher susceptibility to mechanical stress, damage of the myofibers, chronic inflammation, widespread fibrosis, and necrosis [51]. Satellite cells are activated, in an attempt to correct defects in muscle, though this is compromised due the absence or reduction of laminin 211 signals that result in defects in muscle regeneration [9,51].

Mutations in laminin-α2 chain have been reported in other species, including cats and dogs, but the causative effects have been studied mainly in mouse models. Presently, the main mouse models lines studied that recapitulate the main aspects of the human disease are dy^{2j}/dy^{2j}, dy^{W}/dy^{W} *(dyW)*, and dy^{3K}/dy^{3K} [52].The dy^{2j}/dy^{2j} mouse model carries a splice site mutation resulting in a production of a shorter laminin α2-chain and leading to a mild muscular phenotype [52,53]. Postnatal survival can extend over 6 months and this model is often used for studies of peripheral neuropathies and test possible therapeutic approaches [52]. The *dyW* mouse was generated by homologous recombination in embryonic stem cells that resulted in a truncated protein of reduced expression [52,54]. Phenotypically this model presents a severe muscular dystrophy and can survive for up to 12 weeks after birth. The dy^{3K}/dy^{3K} has the most severe phenotype with complete absence of laminin α2-chain surviving only up to 3 weeks after birth [10,52]. Similar to human LAMA2-CMD, the phenotype of the mouse models is characterized by a decreased body mass and peripheral neuropathy in addition to myopathy [10]. Because material for studies of human LAMA2-CMD has mostly been obtained from muscle biopsies [50] the mouse models have further facilitated the understanding of the onset and progression of the disease.

Previous studies in the host laboratory revealed that, in the *dyW* mouse model for LAMA2-CMD, the first defects in LAMA2-CMD occur between embryonic stage 17.5 (E17.5) and E18.5. This period coincides with muscle growth impairment and a reduction in the number of MuSCs and myoblasts [55]. Moreover, there is an overactivation of the STAT3 signaling pathway in *dyW* muscles and the same overactivation was reported in dy^{3K}/dy^{3K} at postnatal day 1 [55,56]. It is thought that the overactivation of this pathway can lead to proliferation and/or differentiation defects [55].

Many approaches have been taken in an attempt to find a cure for LAMA2-CMD. Following recent technological advances, studies have focused on protein and gene therapies [57,58]. Amongst these strategies are the replacement protein therapy with laminin-111 [57], as well as the activation of *Lama1* promoter via CRISPR/Cas9 technology [58]. These strategies are promising but much remains unknown. It is, therefore, important to further understand the details about the mechanisms underlying the disease. This may enable the design of targeted treatments that ameliorate or cure the disease.

1.4. Aim of the project and impact for society

The aim of this thesis, as mentioned above, is to better understand the mechanism underlying the onset of LAMA2-CMD. Previous results from the host laboratory indicate that there is a differentiation defect in *dyW* fetuses [55]. Here the aim was to better understand this defect by using an *in vitro* model for *Lama2*-deficiency in C2C12 myoblasts, which is a cell line established by CRISPR/Cas9 gene editing. The altered levels previously detected in some key myogenic proteins, such as NFIX and MYF5 [59], lead to a better understanding of their cellular behavior in *Lama2*-deficient cells. Due to the previous results associated with overactivation of FAK and STAT3 in the *dyW* mouse models [55], the FAK and STAT3 signaling was modulated in *Lama2*-deficient cells.

As mentioned above, there is no cure or treatment for LAMA2-CMD. LAMA2-CMD patients only receive medical care and surveillance to improve the symptoms. This involves a multidisciplinary support provided by many specialists on neurology, gastroenterology, nutrition, orthopedics,

occupational and physical therapy, speech and language therapy, education, psychiatry, pulmonary medicine, cardiology, ophthalmology, and social work [48].

It is expected that the findings obtained in this project may contribute to our understanding of the primary mechanisms of the onset of LAMA2-CMD, while allowing the discovery of possible targets for the development of therapies that tackle the first events of this incurable disease.

2. Materials and Methods

2.1. Cell Culture

C2C12 cells are an immortalized cell line from adult mouse myoblasts initially obtained by Yaffe and Saxel at the Weizmann Institute of Science in Israel in 1977 [60] and are now commercially available (obtained from DSMZ). The cells were thawed and grown in Dulbecco's Modified Eagle's Medium (DMEM), supplemented with 10 % fetal bovine serum (FBS) and 1 % of an antibiotic mixture: Penicillin (10000 U/mL) and Streptomycin (10 mg/mL) (proliferation medium). The cell lines were maintained in culture at 37 °C, 5 % CO2, constant humidity and when 70 % of confluency was reached, trypsin-EDTA was used to harvest the cells and dilute them for further subculturing.

2.2. CRISPR/Cas9 gene editing and maintenance of the *Lama2*-deficient clones

To generate the *Lama2*-deficient C2C12 cell line, CRISPR/Cas9 gene editing was used. The cells were transfected with two different plasmids containing the Cas9 nuclease each carrying a different guide RNAs (gRNAs) sequence (Vector Builder) (**Table S2** in Annex). A third plasmid expressing GFP was also co-transfected and used for sorting the cells with gRNA/Cas9.

Plasmid mix (0.75 µg plasmid gRNA exon 4, 0.75 µg plasmid gRNA exon 9, 0.5 µg GFP plasmid, 125 µL Opti-MEM and 10 µL P3000 Reagent) was added to a Lipofectamine mix (125 µL Opti-MEM and 5 µL Lipofectamine 3000) during 5 min. In a 6-well plate, 250 µL from the final mix were first added and then 500,000 WT C2C12 cells seeded in each well. The cells were incubated during 48h before FACS sorting using BD FACSAria III in Instituto de Medicina Molecular João Lobo Antunes (IMM). The GFP positive single cells were individually sorted into 96-well plate with DMEM medium supplemented with 20 % FBS and 1 % of Penicillin/ Streptomycin mixture. The single cells were kept in culture, and the formation of a single colony was followed through microscope visualization. Single colonies were then amplified and harvested for validation of the CRISPR/Cas9-editing. All products were purified using the Wizard® SV Gel and PCR Clean-up System (Promega) according to manufacturer's protocol and sent to Sanger sequencing (STAB VIDA, Portugal).

2.3. Drug Treatments

The FAK inhibitor (PF-573228, Sigma-Aldrich) and the STAT3 inhibitor (Stattic, Sigma-Aldrich) were resuspended in dimethylsulfoxyde (DMSO) into a stock concentration of 40 mM and 50 mM, respectively. For each treatment, the final concentration was prepared by diluting in DMEM proliferation medium

2.4. shRNA Cloning

The pLKO.1 cloning vector (**Figure S2** in Annex) is the backbone upon which The RNAi Consortium (TRC) has built a library of shRNAs directed against 15,000 human and 15,000 mouse genes. pLKO.1 is a replication-incompetent lentiviral vector chosen by the TRC for expression of

shRNAs. pLKO.1 can be introduced into cells via direct transfection or can be converted into lentiviral particles for subsequent infection of a target cell line. Once introduced, the puromycin resistance marker encoded in pLKO.1 allows for convenient stable selection [61].

pLKO.1 was digested with EcoRI and AgeI in two sequential digestions due to buffer incompatibility. The first digestion mix (3 µg pLKO.1, 3 µL AgeI, 3 µL 10x Fast Digest Buffer in a total volume of 30 µL) was incubated at 37 ºC for 1 h and then the digested DNA was run in a 1 % agarose gel. The correct band was cut and purified using Promega Wizard™ Genomic DNA Purification Kits. After the first digestion, the second digestion mix (10 µL pLKO.1 digest, 2 µL EcoRI, 2 µL buffer H to a total volume of 20 µL) was also incubated 37ºC for 1 h, followed by a similar gel purification step.

Upon digestion and to increase plasmid efficiency, the pLKO.1 was dephosphorylated using Quick CIP: for each 1 µg of DNA was added 1 µL of Quick CIP, 1.5 µL of buffer 3.1 (NEB) and nuclease free water added until 15 µL. After a 30 min incubation at 37 ºC the reaction was stopped by heat inactivation at 80 ºC for 2 min.

After digestion and dephosphorylation of the pLKO.1 plasmid, the oligos targeting FAK, STAT3 and NFIX were annealed (**Table S2** in Annex). For the oligos annealing step the following mix was prepared: 1 µL of reverse oligo (100 µM), 1 µL of forward oligo (100 µM), 1 µL of 10 x T4 ligation buffer, 0.5 µL of polynucleotide kinase (PNK) enzyme to oligos phosphorylation and 6.5 µL ddH_2O in a total volume of 10 µL. In a thermocycler the oligos were phosphorylated and then annealed using the following parameters: 37 ºC for 30 min, 95 ºC for 5 min and then ramp down to 25 ºC at 5 ºC/min.

The digested plasmid and the annealed oligos were then ligated using the following mix: 1 µL of pLKO.1 digest, 1 µL of a 1:100 dilution of previous annealed oligos, 1.1 µL of 10x T4 ligase buffer, 1 µL of T4 ligase and 5.9 µL of ddH_2O to a final volume of 11 µL. The mix was incubated for 1h at room temperature (RT). In this step a ligation reaction was also carried out containing only the plasmid vector without oligos as a reaction control.

For bacteria transformation, 100 µL of chemically competent NEB® 5-alpha *Escherichia coli* were thawed on ice for 10 min and then 5 µL of the ligation reaction was added to the competent bacteria and the tube carefully flicked 4-5 times to mix bacteria and DNA. The mixture was placed on ice for 30 min. Then, a heat shock was applied at 42 °C for exactly 30 sec. After the heat shock, the mixture was again placed on ice for 5 min. Upon this incubation, 950 µL of Lysogeny broth (LB) were added and the transformed bacteria were incubated at 37 °C for 60 min with vigorous shakinge to recover from chemical transformation and allow time to express the antibiotic (ampicillin) resistance gene present in the plasmids. After incubation, the bacteria were centrifuged, the supernatant was discarded, and the pellet was resuspended in 100 µL of LB. Finally, the resulting mixture was spread on LB agar with ampicillin (100 µg/mL) selection and incubated overnight at 37 °C. The next day, an ampicillin resistance single colony from each plasmid were selected and grown overnight at 37 °C in 10 mL of LB with shake. After bacteria growth, part of the culture obtained was used to make a bacterial stock using 50 % glycerol and another part used to purify the plasmid using GRS Plasmid Purification Kit (GRiSP Research Solutions) according to manufacturer's protocol and sent out for sequencing by Sanger technology (STAB VIDA, Portugal) to confirm the presence of the correct insert.

2.5. Lentivirus Production and shRNA Cells Infection

To access the expression and increase the efficiency of the transfection of the previous generated shRNA, a lentiviral vector that infects dividing and non-dividing cells [62], was used.

Early in the morning the HEK 293T, an immortalized human embryonic kidney cell line, expressing the SV40 large T antigen, was seeded in four T25 flasks to a confluency of 70-80 %. Late in the afternoon the cells were transfected using the calcium phosphate protocol according to the following

procedure: in a 30 mL universal container a mix was done using 4 µg of the lentiviral genome plasmid (shRNA plasmid and a GFP plasmid used as a transfection control), 2 µg Gag-Pol construct, 1 µg Rev, and 1 µg VSV-G (vector-shRNA:Gag-pol:Rev:VSV-G ratio of 4:2:1:1), 100 µL 2.5M $CaCl_2$ and sterile water to 1mL; While bubbling, 1 mL of 2x HSB buffer pH 7.11(**Table S4** in Annex) was added to the DNA/Ca mix, and then the mixture was left for 1 min, to allow the solution to become opalescent; the mixture was then added dropwise to the HEK 293T in the flasks and gently swirled to mix.

In the next day, the growth media from HEK 293T was carefully removed and replaced with fresh DMEM complete media. On the day of the infection, the expression of GFP (expressed by the transfected control plasmid) was visualized under a fluorescence microscope and in case of successful transfection the protocol was continued with the collection of lentiviral particles. The lentivirus-containing media was carefully filtered with a 0.45 µm filter mounted on a syringe to remove of the HEK 293T cells. The supernatant was transferred into a new clean tube, diluted in a 1:3 ratio with growth medium and added to WT and *Lama2*-deficient cells previously plated in T25 flask in order to have a 70 % confluence on the day of infection. In the day after infection the viral supernatant was removed, washed 5 times with PBS and fresh medium was added. Next day the same number of washes with PBS was performed, to further reduce the viral titer and allow further analysis. After washing, the cells were trypsinized and puromycin selection (final concentration of 2.5 µg/mL) was added to the medium for 3 days. After puromycin selection the cells were washed again 5 times with PBS and harvested for western blot analysis (procedure detailed in point 2.8 of Materials and Methods).

2.6. Analysis of Gene Expression

To extract the RNA from WT and *Lama2*-deficient C2C12 cells, 500 µL of TRIzol™ reagent were added to the samples to lyse the cells. Upon dissociation of the nucleoprotein complexes, 100 µL of chloroform was added to separate the lower red phenol-chloroform, the interphase, and the colorless upper aqueous phase. For that, samples were incubated for 2-3 min and centrifuged for 15 min at 12,000 g at 4 °C. The aqueous phase containing the RNA was transferred into a new tube. To precipitate RNA, 250 µL of isopropanol were added to the aqueous phase, and samples were incubated for 10 min. Then the samples were centrifuged for 10 min at 12,000 g at 4 °C. The supernatant was discarded, the pellet was washed twice with 500 µL of 75 % ethanol and centrifuged for 5 min at 7500 g at 4 °C. The ethanol was subsequently removed, the pellet was air dried, resuspended in 20–50 µL of RNase-free water and placed on ice. Samples were then incubated at 55 °C for 10 min and returned to ice. RNA concentrations and quality were determined using Nanodrop1000.

Xpert cDNA Synthesis Kit (GRiSP) was used to synthesize complementary DNA (cDNA) from a single-stranded RNA template. For the reaction (total volume of 20 µL) a mixture containing the following components was prepared: 1µL dNTP mix, 1µL random hexaprimers, 4 µL 5X reaction Buffer with RNA inhibitor (40 U/ µL), 1 µL Xpert RTase (200 U/ µL), RNase free water and 1 µg RNA obtained after RNA extraction. The mixture was mixed thoroughly, briefly centrifuged, and placed in a thermocycler with the following protocol: 25°C for 10 min, 50°C for 50 min and 85°C for 5 min. The cDNA obtained was stored at -20 °C until further analysis by Real-Time qPCR (qPCR). qPCR reaction was performed using Xpert Fast SYBR (Blue) with dye (GRiSP Research Solutions). Reaction mixture of qPCR was prepared with the following components (total of 10 µL per reaction): 5 µL of Xpert Fast SYBR (Blue) (GRiSP Research Solutions) 0.4 µL of forward primers, 0.4 µL of reverse primers and 3.2 µL of nuclease-free H_2O. All reaction components were thawed beforehand, thoroughly mixed and stored on ice, protected from light. Primer sequences used are listed in **Table S2** (Annex). The mixture was then distributed into wells of a 96-well plate and 1 µL of cDNA was added to each well. The plate was sealed with an optically transparent film and centrifuged to remove air bubbles and to ensure that the volume of mixture stayed at the bottom of the well. Each sample was run in duplicate. Finally, a

CFX96^{TM} Real-Time PCR Detection System (Bio-Rad) was used to perform the qPCR reaction using the protocol in **Table S3** (Annex). Data analysis of the PCR run was performed by analyzing the threshold cycle (Ct) values and comparing the Ct value of the gene of interest (GOI) and the housekeeping gene, according to the following equations:

$$\Delta Ct = CT_{\text{housekeeping}} - Ct_{\text{GOI}} \quad (2.1)$$

$$\text{Fold difference to housekeeping} = 2\Delta Ct \quad (2.2)$$

The quality of all qPCR reactions was assessed by melting curve analysis.

2.7. Immunofluorescence and Image Analysis

Approximately 50,000 WT and *Lama2*-deficient C2C12 cells were seeded in 24 well plates with coverslips and incubated for 5 days in proliferation medium. Cells were then washed with 1x PBS, fixed in 4 % paraformaldehyde for 10 min at RT, washed again with 1x PBS and permeabilized for 5 min in 0.1 % Triton in 1x PBS. After washing twice with 1X PBS, cells were blocked for 1h at RT with blocking solution (1 % BSA (bovine serum albumin), 1 % goat serum, 0.05 % Triton-X100, in PBS). Cells were then incubated overnight at 4ºC with primary antibodies diluted in blocking solution (**Table S1** in Annex). On the following day, cells were incubated in secondary antibodies (**Table S1** in Annex), diluted in blocking solution, for 1 h at RT, and were then washed twice with blocking solution. Cells were counterstained with DAPI (4`,6-diamidino-2-phenylindole) for 30 sec, before mounting. Coverslips were removed from the plate, quickly rinsed with water, and left drying for 20-30 min. Mounting media, Mowiol-Dabco (2.5 % 1,4-Diazabicyclo-octane, 10 % Mowiol 4-88, 25 % Glycerol and 0.1 M Tris-HCl) was used to mount coverslips onto slides. Immunofluorescence images were acquired with an Olympus BX60 fluorescence microscope.

2.8. Cell Fractionation

To separate the nuclear and cytoplasmatic fractions a cell fractionation protocol was used. The WT and *Lama2*-deficient C2C12 cells were trypsinizated and centrifuged, the pellets were washed in 1 mL of cold 1x PBS. After centrifugation, the pellet was re-suspended in 150 µL ice-cold buffer A+ (to 10 mL of buffer A (buffer recipe in **Table S5** in Annex) were added 10 µL of 1M DTT, 1x of Roche protease inhibitor cocktail and 75 µL of 10 % Triton) and incubated on ice for 5 min. The samples were centrifuged 5 min at 1300 g at 4 ºC, the supernatant (S1) containing the cytoplasmic proteins, was cleared by centrifugation for 20 min at 20,000 g at 4ºC, the supernatant (S2) was kept and 150 µL of 2x SDS-PAGE sample buffer (20 % Glycerol, 4 % SDS 100 mM, Tris pH 6.8, 0.2 % Bromophenol blue, and 100mM DTT) were added. The pellet (P1) containing the nuclei was washed twice with 500 µL from buffer A+, centrifuged 5 min at 1300 g at 4 ºC and resuspended in 100 µL of 2x SDS-PAGE sample buffer.

2.9. Western Blot and Protein Analysis

Both samples obtained from the cell fractionation or whole cells extracts were processed and analyzed by western blot. For whole cell extracts, cells were harvest directly in 75 µL of 2x SDS-PAGE sample buffer. To degrade DNA and RNA, fractionation samples and whole cell extracts were incubated with benzonase at room temperature for 20 min or disrupted using tissue lyser (Retsch MM400 Tissue Lyser) during 2 min x2 (frequency 30/sec). Samples were heated at 50 °C for 10 min and centrifuged at

maximum speed for 15 min. The supernatant was transferred into a new microcentrifuge tube and protein concentration was quantified using Nanodrop1000 measuring the absorbance at 280 nm. The samples were stored at -20 °C until further use.

Since the proteins under study ranged between 17-125 kDa, 10 % polyacrylamide gels were used to separate the proteins by size. Samples were loaded in the gel (approximately 25/30 µg of protein) and then run in 1x Running Buffer (3.02 g Tris base, 14.42 g Glycine, 1 g SDS in 1 L distilled water) for 1 h at 150 V, using the Mini-PROTEAN® Tetra electrophoresis system (Bio-Rad). Next, a transfer cassette was mounted with the gel and a polyvinylidene fluoride (PVDF) membrane, previously activated with methanol. The Mini Trans-Blot® Cell (Bio-Rad) was used for protein transfer with chilled Transfer Buffer (5.82 g Tris, 2.93 g glycine in 1 L distilled water) for 45 min at 100V. After the transfer, to confirm the quality of protein extracts and verify the loading of the gel, GelCodeTM Blue Safe Protein Stain (ThermoFisher Scientific) was used to stain the gel for 1 h. Next, membranes were blocked for 1 h in 5 % powdered milk in TBST (20 mM Tris, 150 mM NaCl, 0.1 % Tween20 and distilled water, pH 7.4-7.6), with agitation. Membranes were rinsed 3 times in TBST and incubated with the primary antibody, diluted in 2 % BSA and 0.02 % Sodium Azide in TBST overnight at 4 °C, with agitation (antibodies and dilutions used are listed in **Table S1**, Annex). On the following day, membranes were incubated with secondary antibodies coupled with horseradish peroxidase (HRP) diluted in 5 % powdered milk in TBST for 1 h at RT, after being previously washed in TBST. After incubation, membranes were washed 3 times, for 5 min each, in TBST and chemiluminescence was detected using SupersignalTM West Pico Chemiluminescent Substrate HRP (ThermoFisher Scientific). Images were acquired using the Amersham Imager 680 RGB (GE Healthcare).

2.10. Statistical Analysis

ImageJ (Image Processing and Analysis in Java) was the software used to quantify the bands from western blot analysis and immunofluorescence image analysis. GraphPad Prism 8 was the software used for statistical analysis. Unpaired t-test was used to compare two groups, one-way ANOVA was used to compare two or more groups and two-way ANOVA was used for multiple comparisons between groups. Serial cloner 2.6.1, SnapGene software and Synthego Performance Analysis, ICE Analysis (2019.v3.0) were used for sequencing analysis.

3. Results

3.1. *Lama2*-deficient C2C12 myoblast cell lines- generation and validation

To study the mechanisms altered during the onset of LAMA2-CMD, the host laboratory established an *in vitro* model, a *Lama2*-deficient myoblast C2C12 cell line (KO) using CRISPR/Cas9 gene editing [63]. Since these cell lines rapidly lose their ability to proliferate in culture, there is a constant need to generate new clones. For that, three plasmids were used, two expressing each a different gRNA that targeted exons 4 and 9 of *Lama2* gene and one expressing the selection GFP marker. The selection of two targeted exons was a strategy used to improve the KO success, since one of the exons, for many reasons, may not be altered (**Figure 3.1A**). The transfected cells were analyzed by flow cytometry and 16,3% of the cells were found to be GFP positive cells and were subsequently single-cell sorted into 96-well plates. After that, single cells were kept in culture to be expanded and pellets of the cells were collected. RNA was extracted from these cell pellets, cDNA was synthesized and qPCR for *Lama2* mRNA analysis was performed. From the analyzed clones, four of them showed absent or reduced *Lama2* mRNA expression (KO7, KO8, KO15 and KO26) (**Figure 3.1B**). The clone *Lama2* KO7 was the one selected to proceed with further analysis. The reduced expression of *Lama2* gene in clone KO7

was further confirmed by qPCR analysis in three independent experiments (**Figure 3.1C**) and the targeted genomic regions (exon 4 and 9) were sequenced and analyzed. In exon 4 sequencing, after the protospacer adjacent motif (PAM) sequence, a nucleotide was inserted, changing the open reading frame (**Figure 3.1D**, left). The exon 9 sequencing had some background, several additional peaks are observed across the sequence and not just in the cut site which difficulted the sequence analysis (**Figure 3.1D**, right). Furthermore, it was found that target gRNA exon 9 used was designed for the recent mouse genomic sequence, which shows some differences when compared to the sequence of WT C2C12 cells (**Figure S1** in Annex), and Synthego analysis was not possible. After qPCR analysis and Sanger sequencing, the C2C12 KO7 cell line was assumed as *Lama2* KO according to the phenotype behavior such as increased levels of P-STAT3 and heme-oxygenase 1 (HO-1) (**Figure 3.1E, F**) similar to the previous clones and the confirmed alterations in exon 4.

All the experiments presented below were performed using at least two *Lama2* KO single cell clones, KO7 (generated in this study) and KO5 or KOE, which were previously generated [63]. The use of two independent cell clones guarantees that the alterations observed are caused by *Lama2*-deficiency and are not due to other characteristics of the clone under study.

A.

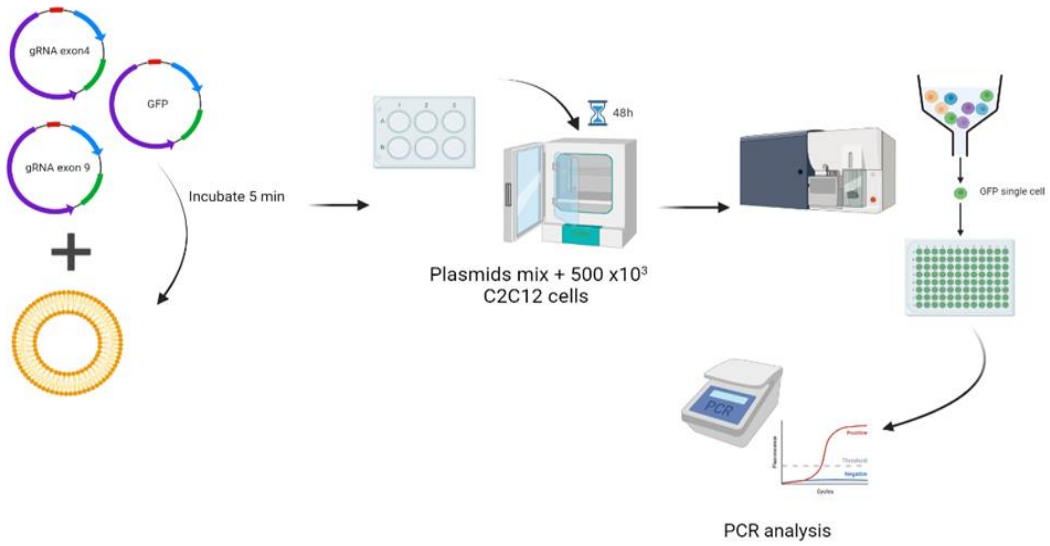

B.

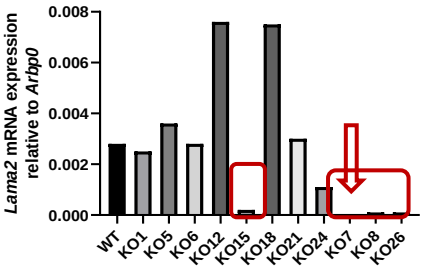

C.

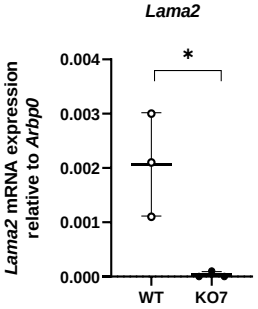

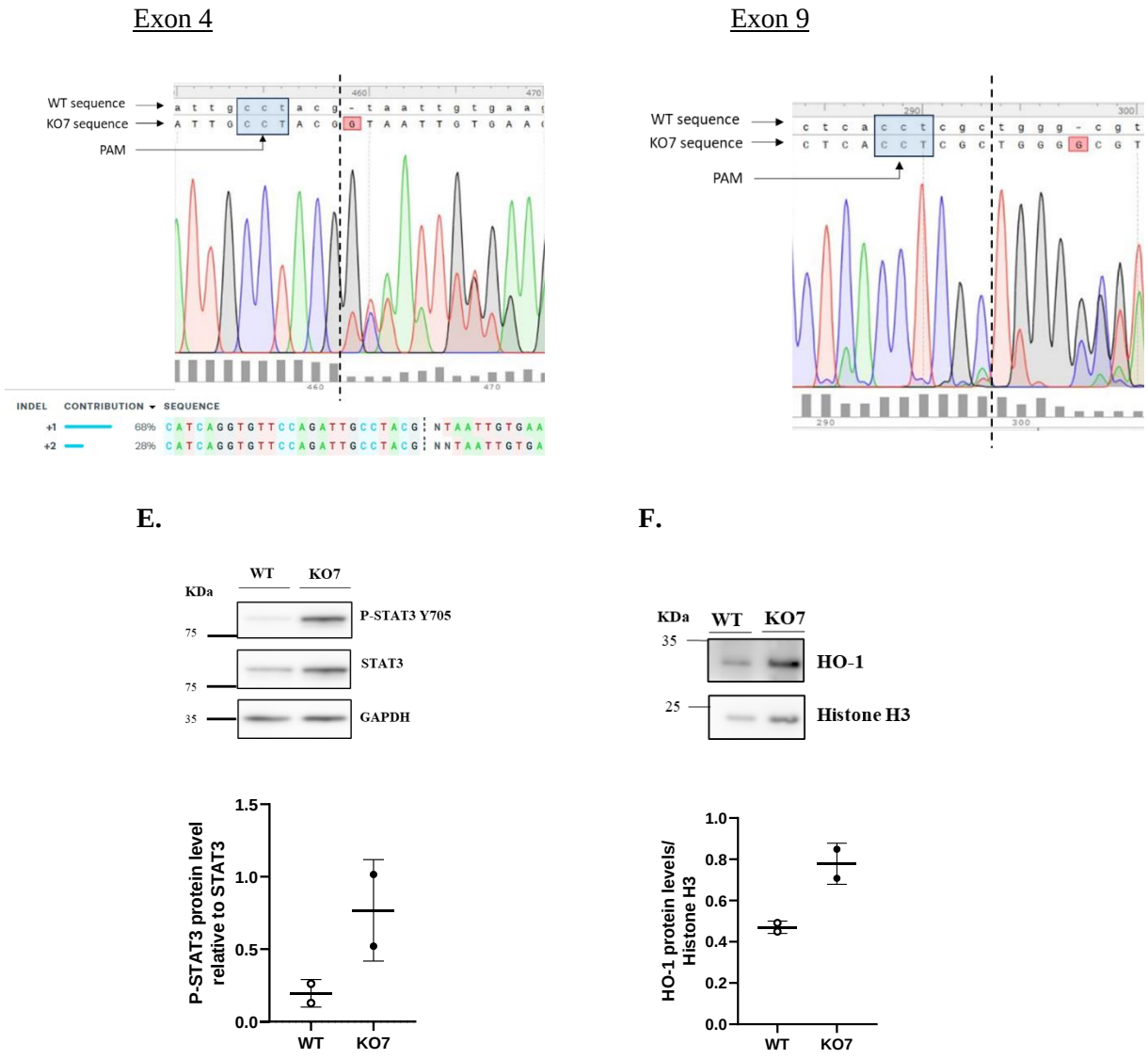

Figure 3.1 – Generation and characterization of *Lama2* KO C2C12 cell lines. A. C2C12 cell line was transfected using lipofectamine with three plasmids. Two plasmids allowing *Lama2* knockout mediated by CRISPR/Cas9, each one having a gRNA specifically targeting exon 4 or exon 9 of *Lama2*. The third plasmid encoded GFP, allowing the selection of positively transfected cells by fluorescence activated cell sorting (FACS). GFP positive cells were individually sorted into 96-well plates to generate single cell clones. Validation of efficient deletion was performed by qPCR analysis. Image created in BioRender.com. **B.** Relative expression of *Lama2* mRNA levels in transfected C2C12 cells as described in (**A**) was analyzed by qPCR. Transcript levels were normalized with the housekeeping gene *Arbp0/Rplp0*. Red square indicates the C2C12 cell lines with reduced *Lama2* mRNA expression. Red arrow indicates the C2C12 KO cell line selected to proceed with further analysis. n=1 experiment. **C.** qPCR relative expression levels of *Lama2* mRNA in the C2C12 KO7 cell line. Transcript levels were normalized with the housekeeping gene *Arbp0/Rplp0*. Statistical analyses were performed using the unpaired t-test, *p-value < 0.05. Each dot represents an individual sample, n=3 independent experiments. **D.** Sanger sequence alignment of WT and the single cell clone KO7 amplified with exon4_Fwd (left) and exon9_Rev (right) primers (see **table S2** in annex). The black square indicates the PAM site, and the red squares indicates the nucleotide insertions in KO7 sequence. The vertical black dotted line represents the actual cut site. The contributions in the Sanger data analysis show the inferred sequences present in the edited population and their relative proportions. The alignments and the analysis of the Sanger data were performed using the SnapGene software (**D**) and Synthego Performance Analysis, ICE Analysis. 2019. v3.0 (**D, left panel**). **E.** Representative western blot analysis of STAT3 phosphorylation on tyrosine 705 (P-STAT3 Y705) in *Lama2* KO7 cell line. GAPDH was used as loading control (top). Densitometry analysis of the WB (bottom). P-STAT3 protein levels were normalized to STAT3. n=2 independent experiments. **F.** Representative western blot analysis of heme-oxygenase 1 (HO-1) in *Lama2* KO7 cell line. Histone 3 (H3) was used as loading control (top). Densitometry analysis of the western blot (bottom). HO-1 protein levels were normalized to H3. n=2 independent experiments

3.2. Myoblast differentiation is compromised in *Lama2* C2C12 KO cell lines

Previous unpublished results from the host laboratory had shown that, in the absence of *Lama2* gene, the differentiation of myoblasts is impaired when the cells were in cultured for 5 days in differentiation medium (containing 2 % horse serum). However, since the differentiation medium has low levels of serum (only 2 % serum in contrast to proliferation medium that has a total of 10 % fetal bovine serum, which promotes differentiation and reduces proliferation), the proliferation defects could have accentuated in KO cell lines, possibly impacting the generation of the initial number of cells necessary for the differentiation to properly occur. Thus, the experiment was repeated using proliferation medium. Cells cultured in proliferation medium reached a high confluency, which prompted them to exit the cell cycle and undergo differentiation leading to the formation of myosin heavy chain-positive multinucleated myofibers [64]. To compare the differentiation capacity of WT and *Lama2 KO* cell lines, an immunofluorescence analysis labelling myosin heavy chain, as differentiation marker, after 5 days in proliferation medium, was performed. In agreement with the previous results, myofibers formation was compromised in *Lama2* KO cells, while in WT cells cultured for the same amount of time (day 5) elongated and aligned multinucleated myofibers are formed (**Figure 3.2A**). The number of fibers per nuclei was quantified and showed a significant reduction in *Lama2* KO cell lines (**Figure 3.2B**). Moreover, the number of nuclei per myosin positive cell was also greatly reduced in the *Lama2* KO cells (**Figure 3.2C**). Myogenin acts as transcriptional activator in muscle differentiation promoting the transcription of target genes in muscle, the levels of *Myog* and its target genes *Tubb6* (Tubulin Beta 6 Class V) and *Myl1* (Myosin Light Chain 1) was analyzed. On day 5 of culture, *Myog* mRNA expression is decreased in *Lama2* KO cells and so is the mRNA expression of *Tubb6* and *Myl1* (**Figure 3.2D**).

A.

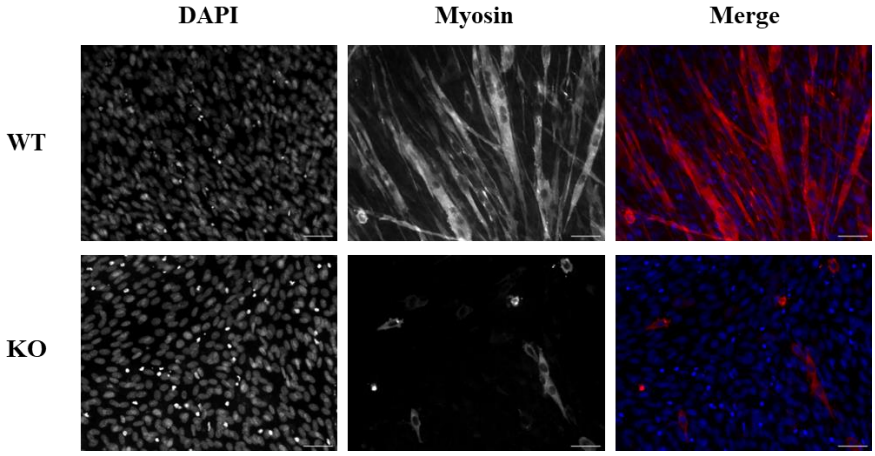

B.

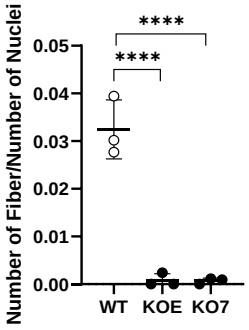

C.

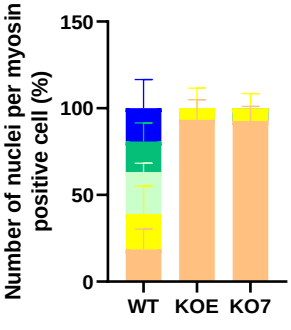

Nuclei	WT vs. KO7	WT vs. KOE
1	p < 0.0001	p < 0.0001
2	p = 0.2038	p = 0.1709
3	p = 0.0069	p = 0.0069
4	p = 0.0605	p = 0.0605
4+	p = 0.0368	p = 0.0368

D.

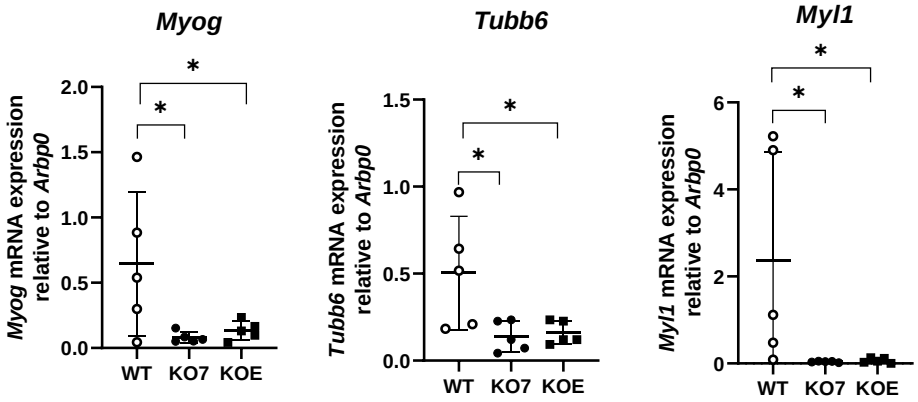

Figure 3.2- *Lama2* KO C2C12 cell lines form few and aberrant myotubes. A. Representative immunofluorescence image of WT and *Lama2* C2C12 KO cell lines on day 5 of cultured in proliferation medium. Anti-myosin heavy chain antibody was used to label myotubes (red). Nuclei were counterstained with DAPI (blue). Scale bars: 50 µm. **B.** Immunofluorescence analysis of the number of fibers per number of nuclei in WT and in two independent *Lama2* KO C2C12 (KO7 and KOE) single cell clones. Only myosin positive cells with two or more nuclei were considered as fibers. Statistical analysis were performed using ordinary one-way ANOVA, ****p-value < 0.0001. Each dot represents an individual sample, n= 3 independent experiments. **C.** Immunofluorescence analysis of the number of nuclei present in each myosin-positive cell in WT and two independent *Lama2* KO single cell C2C12 (KO7 and KOE), shown in percentage. The different colors in bars represent the number of nuclei present in a single myosin positive cell. Five different groups were analyzed, myosin positive cells with 1, 2, 3, 4 or more than 4 nuclei were quantified separately. n= 3 independent experiments. Statistical analysis was performed using two-way ANOVA for each number of nuclei per myosin positive cell. **D.** qPCR relative expression levels of *Myog, Tubb6* and *Myl1* mRNA in C2C12 KO cell lines. Transcript levels were normalized with the housekeeping gene *Arbp0/Rplp0.* Each dot represents an individual sample, n=5 independent experiments.

3.3. Nuclear NFIX levels were increased in *Lama2* KO C2C12 cell lines, while nuclear MYF5 levels were reduced

Cell fractionation is a biochemical process that separates different cellular fractions, including nuclear and cytoplasmatic fractions, and is a useful technique to study the cellular localization of the proteins under study. Previous results from the host laboratory revealed that NFIX and MYF5 were altered in *Lama2* KO cell lines when compared to WT samples [59] , and YAP revealed a tendency to be less expressed in KO cells when compared to WT cells (unpublished data). To assess if the localization of these transcription factors is altered in *Lama2* KO cells, a cell fractionation method was used, and cell fractions were then analyzed by western blot (WB). The nuclear and cytoplasmatic fractions were separated and YAP, MYF5 and NFIX protein levels were analyzed. Exclusive cytoplasmic and nuclear markers were used to confirm the correct separation of the fractions. Vinculin was used as cytoplasmic marker since it is a cytoplasmic actin-binding protein enriched in focal adhesions and adherence junctions [65]. The histones are nuclear proteins responsible for chromosomal structural support [66] and histone H3 was selected as nuclear marker. In the western blot analysis, it was difficult to identify the correct band corresponding to the YAP protein (expected size 65 KDa) in both nuclear and cytoplasm fractions, since in different western blot analysis the band had different sizes (**Figure 3.3A**) and therefore no quantitative analysis was performed. In the nuclear fraction, MYF5 levels were significantly reduced in *Lama2* KO cells contrarily to what was observed for NFIX levels that were highly increased in *Lama2* KO cell lines (**Figure 3.3B**). NFIX is significantly increased in the cytoplasmic fraction of *Lama2* KO cells (**Figure 3.3C**), while MYF5 protein remains unaltered, suggesting that it is retained in the cytoplasm and, for some unknown reason, cannot go into the nucleus in *Lama2* KO cells (**Figure 3.3C**).

A.

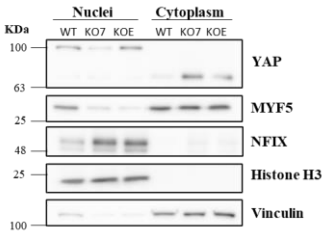

B.

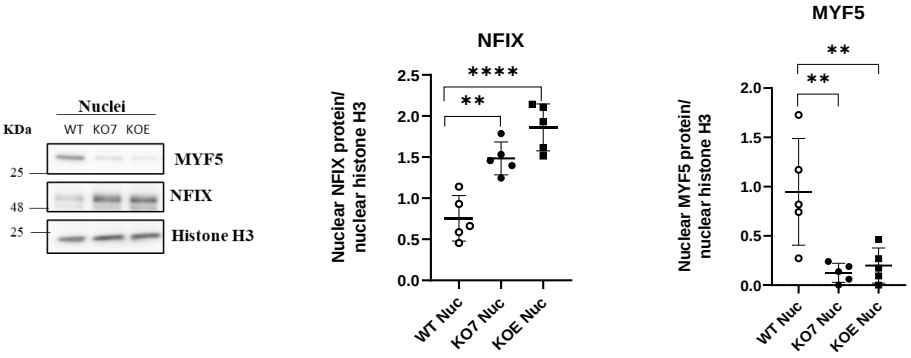

C.

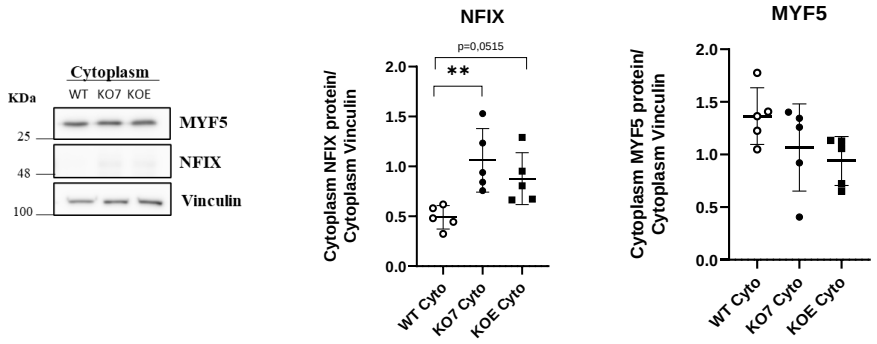

Figure 3.3- Cell fractionation revealed different proteins localization in *Lama2* KO cell lines when compared to the WT C2C12 cell line. A. Representative western blot image of proteins in nuclei and cytoplasmatic fractions in WT and in two independent single cell *Lama2* KO C2C12 cell lines (KO7 and KOE). A cell fractionation protocol was used to separate both fractions (nuclear and cytoplasmic). Histone H3 (H3) was used as a nuclear marker and vinculin as a cytoplasmic marker. **B.** Nuclear fraction densitometry analysis of protein levels in (**A**). Nuclear protein levels were normalized to Histone H3. Statistical analysis was performed using ordinary one-way ANOVA, **p-value < 0.01, ****p-value < 0.0001. Each dot represents an individual sample, n= 5 independent experiments. Nuc – nuclear fraction. **C.** Cytoplasmic fraction densitometry analysis of protein levels in (**A**). Cytoplasmic proteins levels were normalized to vinculin. Statistical analysis was performed using ordinary one-way ANOVA, **p-value < 0.01. Each dot represents an individual sample, n= 5 independent experiments. Cyto – cytoplasmatic fraction.

3.4. Pharmacological FAKi treatment reduces P-FAK and P-STAT3 protein levels in WT and *Lama2* KO C2C12 cell lines

Previous results from the host laboratory showed an increased in the levels of phosphorylated FAK (P-FAK) in *dyW* muscles at E17.5 (unpublished data). It hypothesized that this may be related with the impairment in fiber formation of *Lama2*-deficient cells compared to the WT cells after days in proliferation medium. In the attempt to revert this effect and find the optimal concentration, WT and *Lama2* KO cells were incubated with FAK inhibitor (FAKi) PF-573228 for 2 days. Based on the literature [29], three concentrations were selected (2 µM, 1 µM and 0.5 µM) and the cells were observed using a brightfield microscope. A reduction in cell survival was observed in cells treated with the highest concentration (2 µM) and no difference was observed in the lower concentrations (1 and 0.5 µM) compared to untreated control (C) cells (**Figure 3.4.1A**). The cells treated with 1 µM and 0.5 µM of FAKi were analyzed by western blot and a reduction in P-FAK was observed in WT and KOE cells treated with FAKi 1 µM (**Figure 3.4.1B**).

Considering that the differentiation analysis would involve periods of 5 days of culture, the treatment with FAKi was prolonged to 3 days of incubation and a new concentration (0.75 µM) was tested. The cells incubated with FAKi were observed in a brightfield microscope, and they were phenotypically identical to the respective controls (**Figure 3.4.1C**). In western blot analysis, a tendency for P-FAK levels to be reduced in WT and KOE was observed in both concentrations (0.75 and 1 µM), while only in concentration 0.75 µM in case of KO5 (**Figure 3.4.1D**). Also, some alterations were observed in the total FAK in **Figure 3.4.1B, D** when normalized to the respective loading control GAPDH or Vinculin.

A.

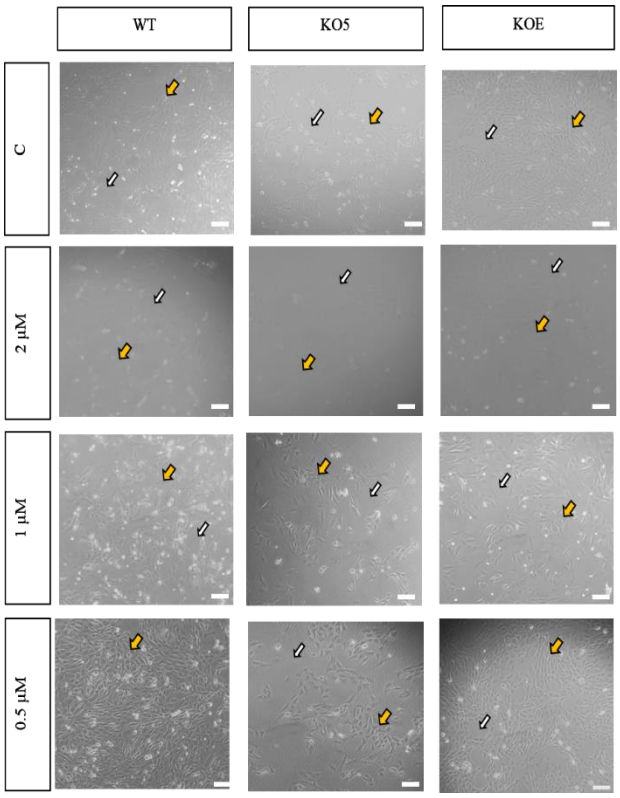

B.

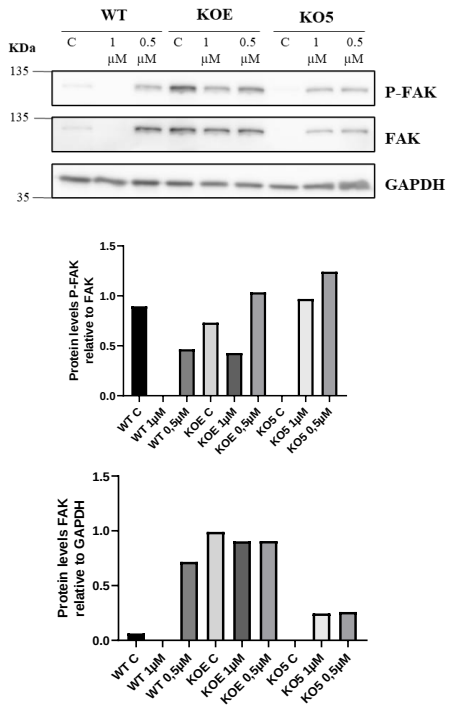

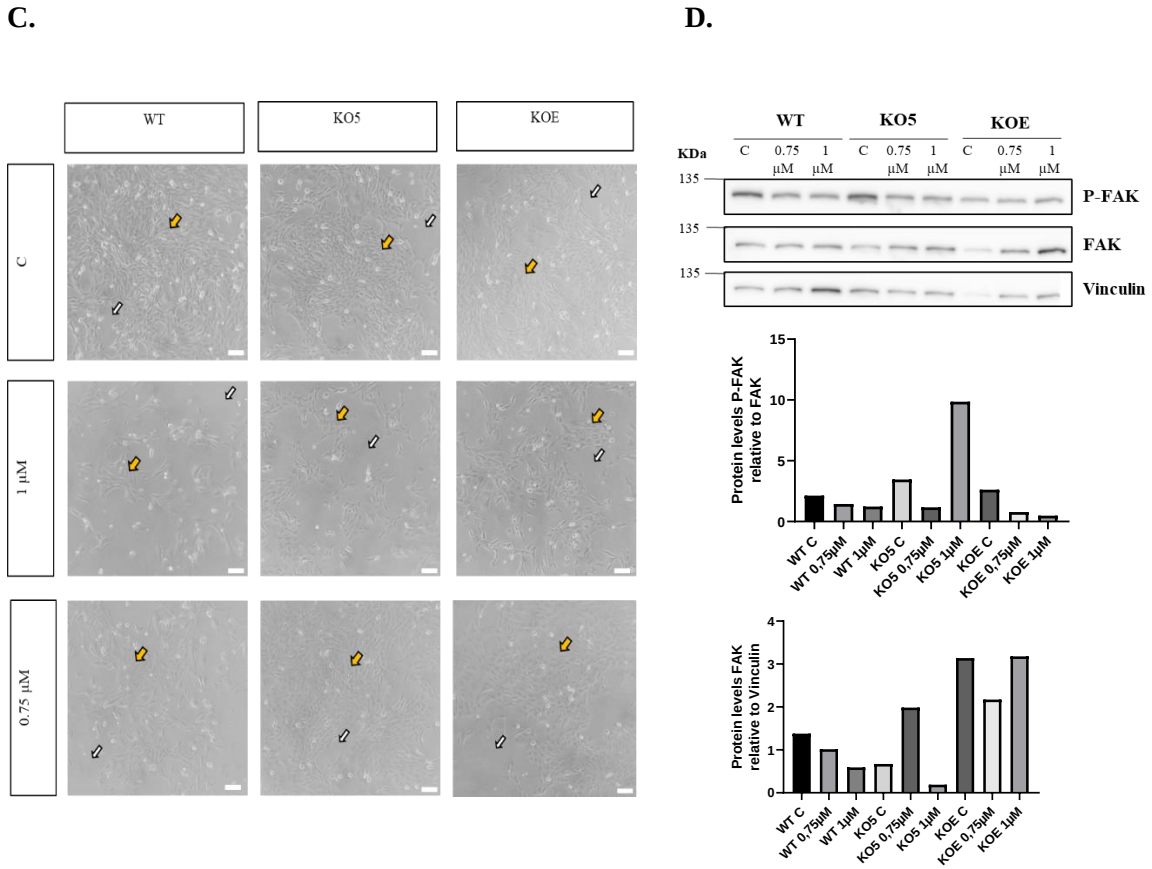

Figure 3.4.1 – Optimization of long-term FAK inhibitor treatment in WT and *Lama2* KO C2C12 cell lines. A. Representative brightfield microscopy images of WT and two independent single cell *Lama2* KO C2C12 cell lines (KO5 and KOE) treated with different concentrations (0.5; 1 and 2 µM) of FAK inhibitor (PF-573228) in cell proliferation medium for 2 days (2d). White arrows indicate absence of cells. Yellow arrow indicates presence of cells. Scale bar = 100 µm **B.** Western blot analysis of FAK phosphorylation on tyrosine 397 (P-FAK Y397) in cells treated as described in (A.). GAPDH was used as loading control. Respective densitometry analysis of the western blot images is shown below. P-FAK protein levels were normalized to FAK and FAK protein levels were normalized to GAPDH. n=1 independent experiments **C.** Representative brightfield microscopy images of WT and two independent single cell *Lama2* KO C2C12 cell lines (KO5 and KOE) treated with different concentrations (0.75 and 1 µM) of FAK inhibitor (PF-573228) in cell proliferation medium for 3 days (3d). White arrows indicate absence of cells. Yellow arrow indicates presence of cells. Scale bar = 100 µm **D.** Western blot analysis of P-FAK Y397 (Tyrosine 397) in cells treated as describe in (C.). Vinculin was used as loading control. Respective densitometry analysis of the western blot images is shown below. P-FAK protein levels were normalized to FAK and FAK protein levels were normalized to Vinculin. n= 1 independent experiments. C – control.

Since the long-term FAKi treatment gave inconclusive results because of the observed dose-response relationship, a short-term treatment was adopted. 30 minutes (30 min) and 2 hours (2 h) were chosen as time-points with two FAKi concentrations (1 µM and 3 µM) based on the literature [29,67] and on previous results. Compared to the long-term treatments, the western blot analysis of the short-term points revealed alterations in total FAK expression when normalized to control GAPDH (**Figure 3.4.2A**) suggesting that the inhibitor is affecting the total FAK levels when it should only affect the phosphorylation of FAK [67]. Therefore, from this point on, the P-FAK levels were also normalized to the GAPDH levels. The strongest and more consistent reduction of P-FAK was observed on cells treated with 3 µM FAKi for 2 h (**Figure 3.4.2B**). Therefore, this time-point was considered the optimal condition to reduce P-FAK levels in *Lama2* KO C2C12 cell lines.

A.

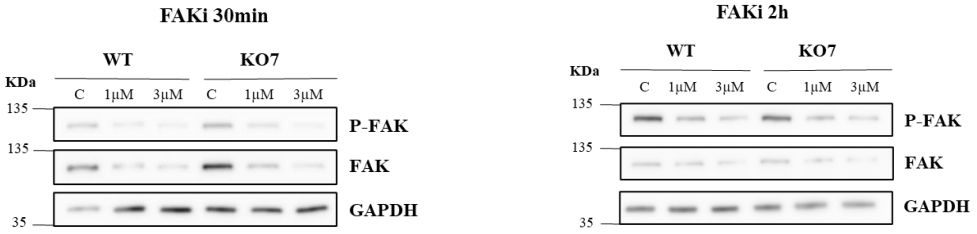

B.

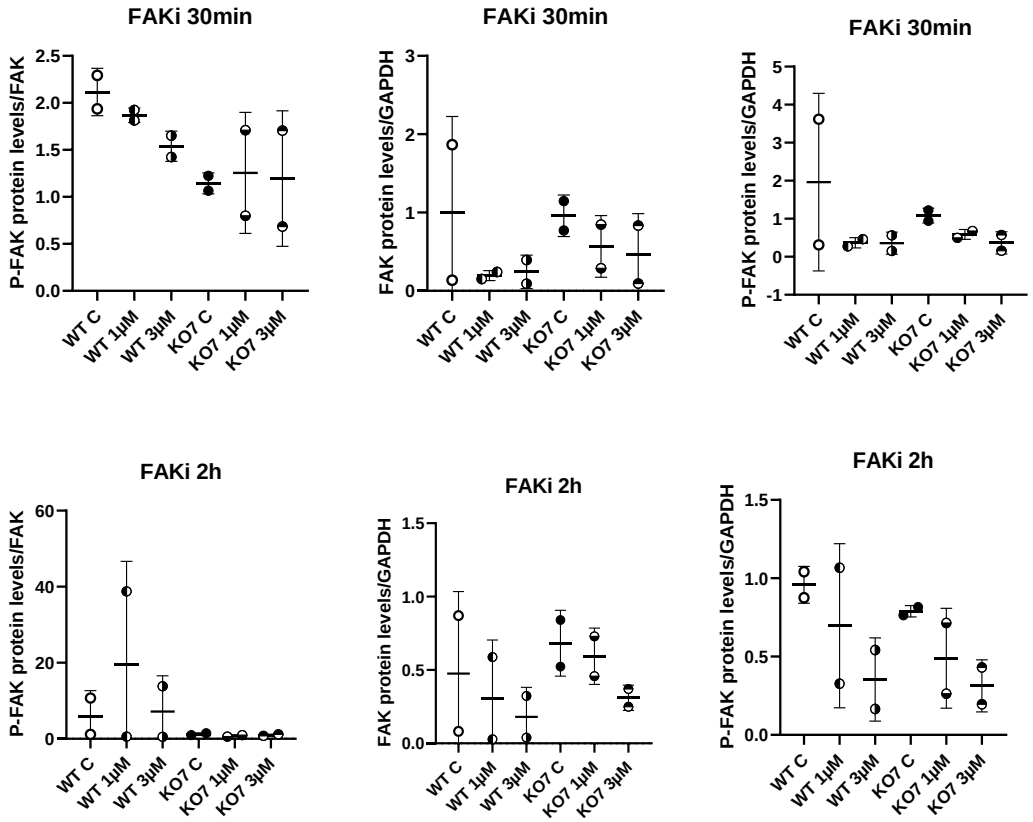

Figure 3.4.2 – Optimization of short-term FAK inhibitor treatment using WT and *Lama2* KO C2C12 cell lines. A. Representative western blot analysis of P-FAK Y397 (Tyrosine 397) in WT and one independent C2C12 *Lama2* single cell KO (KO7) treated with two different concentrations (1 and 3 μM) of FAK inhibitor (FAKi) (PF-573228) in cell proliferation medium for 30 minutes (30 m) or 2 hours (2 h). GAPDH was used as loading control. **B.** Densitometry analysis of the western blot images in (**A**). P-FAK levels were normalized to FAK and GAPDH, n=2 independent experiments.

When the number of experiments was increased, the tendency for P-FAK levels to be reduced was observed in FAKi treated compared to untreated control in all cell lines (**Figure 3.4.3A, B**), while levels of total FAK did not show a specific tendency (**Figure 3.4.3C**). Nevertheless, the reduction in P-FAK was not significant since one of the sets analyzed showed high protein levels when compared to the other sets. To overcome that issue, all conditions were normalized to the ratio of P-FAK/GAPDH of each WT control (C) experiment. The reduction of P-FAK levels in *Lama2* KO cell lines treated with FAKi was significant when compared to the untreated controls. Since the WT C P-FAK levels were normalized to themselves, the ratio is equal to 1 which explains the fact that by using a one-way ANOVA

statistical test (which measures variance), there is no significant differences between treated and untreated in the case of WT. In this case, a t-test was used, and WT treated with FAKi showed a significant decrease of P-FAK levels when compared to untreated control (p value < 0.0001) (**Figure 3.4.3D**).

Having established the FAKi treatment conditions, other proteins were analyzed to assess if the decrease in P-FAK levels could ameliorate the phenotype of *Lama2* KO cells. P-STAT3, as mentioned before, is overexpressed in *Lama2* KO cell lines. To assess if this pathway is regulated by FAK pathway, P-STAT3 levels were analyzed. The results showed a tendency for a decrease in P-STAT3 levels in cells treated with FAKi, particularly in the WT (**Figure 3.4.3A, E-G**). Oxidative stress is another marker associated with *Lama2*-deficiency. To analyze if inhibition of P-FAK ameliorates this condition, heme oxygenase-1 (HO-1) was analyzed and no reduction was observed in cells treated with FAKi (**Figure 3.4.3A, H**). Finally, NFIX was observed to be increased in both nucleus and cytoplasm in *Lama2*-defient cells, but there were no effects of FAKi on this pattern (**Figure 3.4.3A, I**).

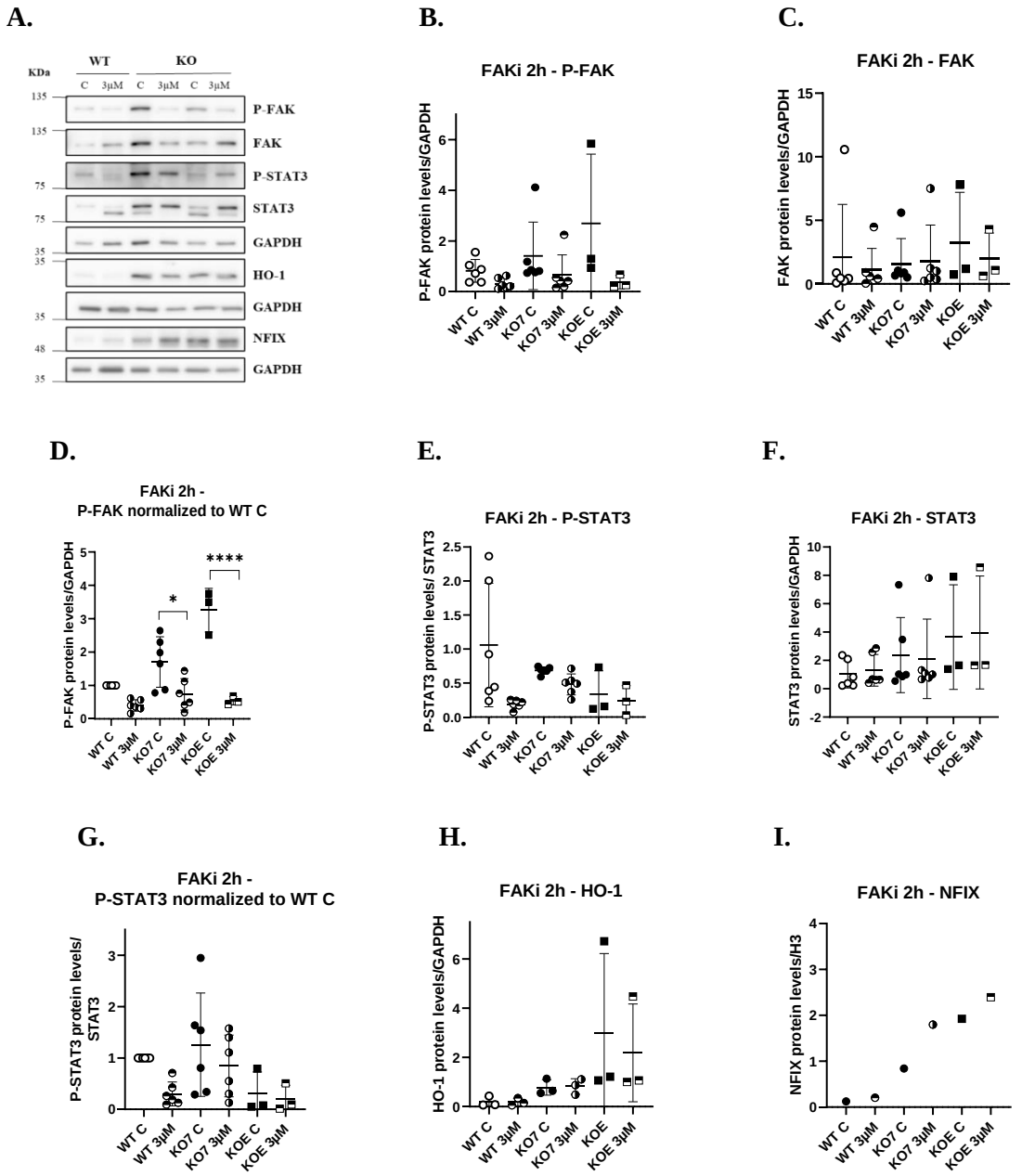

Figure 3.4.3 – Effect of short-term FAKi treatment on other protein markers. A. Representative western blot analysis of P-FAK Y397 (Tyrosine 397), P-STAT3 Y705 (Tyrosine 705) and HO-1 in WT and two independent C2C12 *Lama2* single cell KO (KO7 and KOE) treated with FAKi 3 µM for 2 h. GAPDH was used as loading control. **B-H.** Western blot protein densitometry analysis from (**A**). P-FAK (**B**) and FAK (**C**) protein levels were normalized to GAPDH. P-FAK levels normalized to GAPDH were additionally normalized to the WT control from each experiment (**D**). P-STAT3 protein levels were normalized to STAT3 (**E**), STAT3 protein levels were normalized to GAPDH (**F**). P-STAT3 levels normalized to STAT3 were additionally normalized to the WT control from each experiment (**G**). HO-1 protein levels were normalized to GAPDH (H). Statistical analysis was performed using an ordinary one-way ANOVA, *p-value < 0.05, ****p-value < 0.0001. Each dot represents an individual sample, n= 3-6 independent experiments. **I.** Western blot protein densitometry analysis from (**A**). NFIX protein levels were normalized to H3. Each dot represents an individual sample, n= 1 independent experiments.

Moreover, to assess if the inhibition of FAK ameliorate the compromised myofibers formation in *Lama2*-deficiency, cells were treated with FAKi on the 5 days of culture with proliferative medium, as described before for the differentiation protocol. The FAKi treatment was applied on day 2 and day 4 during 2 h and no differences were observed in myofibers compared to respective untreated controls (**Figure 3.4.4**).

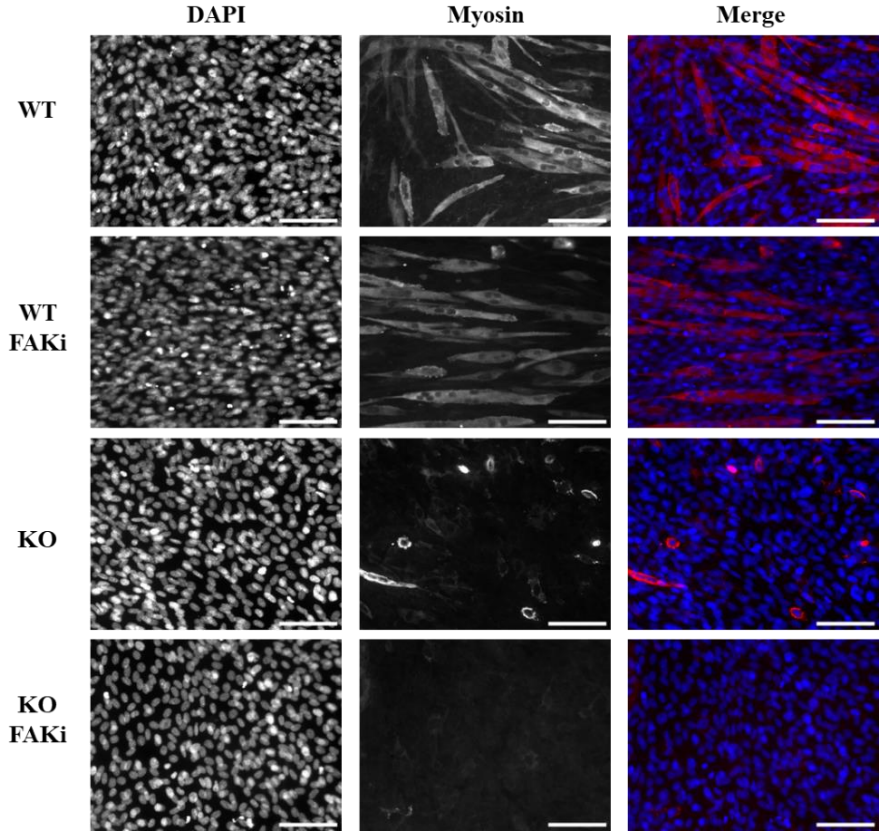

Figure 3.4.4 –FAKi treatment effect into myofibers formation. A. Representative immunofluorescence image of WT and *Lama2* C2C12 KO cell lines on day 5 of cultured in proliferation medium. The cells were pre-treated with FAKi 3 µM 2h on day 2 and day 4 of the 5 days cells cultured. Anti-myosin heavy chain antibody was used to label myotubes (red). Nuclei were counterstained with DAPI (blue). Scale bars: 50 µm.

3.5. Pharmacological STAT3i treatment in WT and *Lama2* KO C2C12 cell lines

Considering that P-STAT3 levels were also increased in *Lama2* KO cells and in *dyW* muscle at E17.5, KO and WT cell lines were treated with the STAT3 inhibitor (STAT3i) Stattic [68], using the same methodology as for FAKi. After 3 days of incubation with high concentrations (5, 2.5 and 1 µM) the cells were observed in a brightfield microscope and had not survived. At a lower concentrations (0.5

and 0.25 µM) no differences were observed in terms of survival and general morphology of the cells (**Figure 3.5A**). However, no differences in P-STAT3 levels were observed in western blot analysis with 0.5 and 0.25 µM concentrations of STAT3i (**Figure 3.5B, C**).

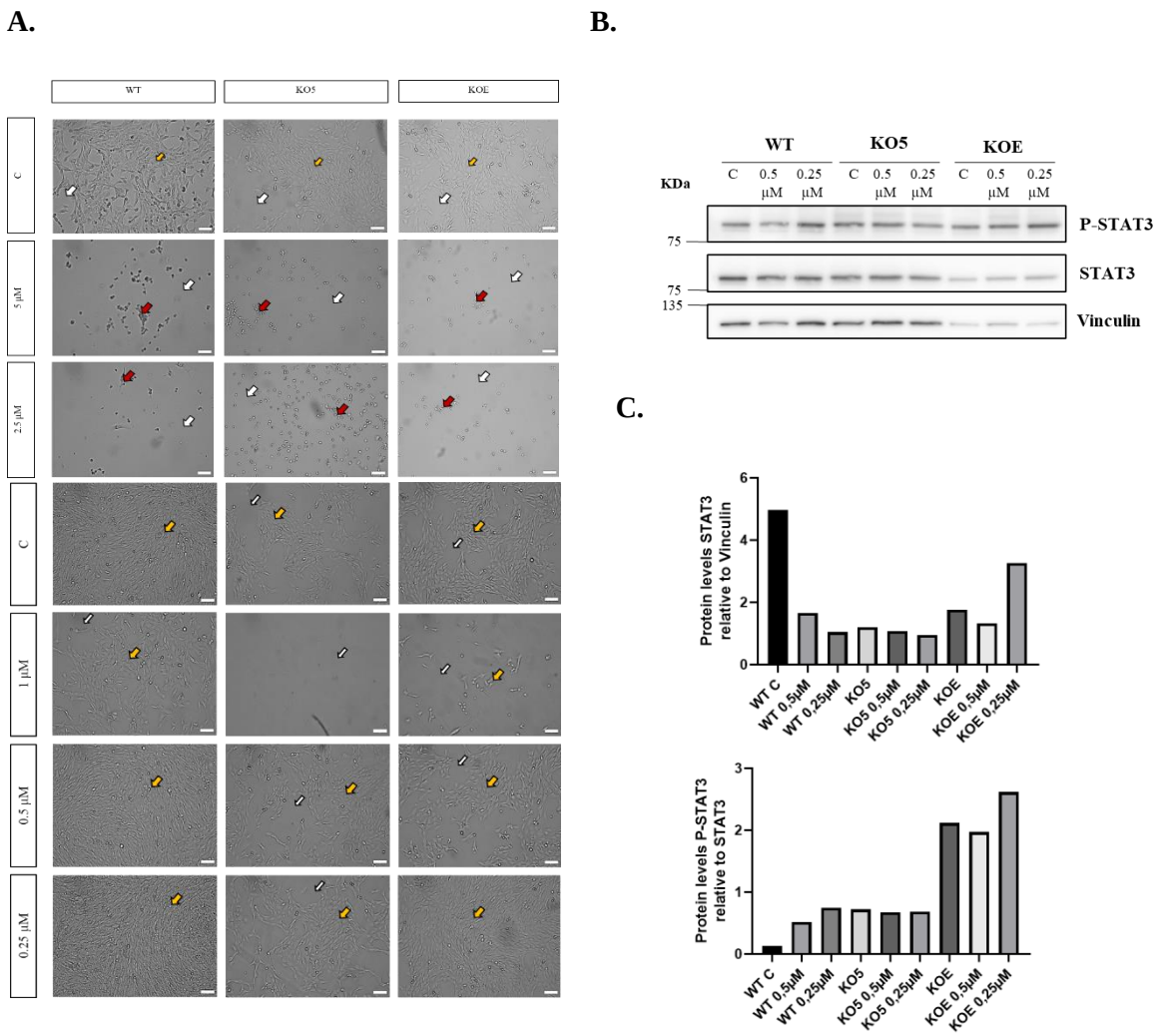

Figure 3.5.1 – Optimization of STAT3 inhibitor treatment using WT and *Lama2* KO C2C12 cell lines. A. Representative brightfield microscopy images of WT and two independent *Lama2* single cell KO C2C12 cells (KO5 and KOE) treated with different concentrations (0.25; 0.5; 1; 2.5; and 5 µM) of STAT3 inhibitor (Stattic) in cell proliferation medium for 3 days. White arrows indicate absence of cells. Yellow arrow indicates presence of cells. Red arrow indicates dead cells. Scale bar = 100 µm **B.** Western Blot analysis of STAT3 phosphorylation on tyrosine 705 (P-STAT3 Y705) in cells treated as described in (**A**). Vinculin was used as loading control. **C.** Densitometry analysis of the WB images shown in (**B**). P-STAT3 protein levels were normalized to STAT3 and STAT3 protein levels were normalized to Vinculin. n= 1 experiment. C- control.

Similar to what was found for the FAKi treatment, where long-term treatment was not possible, a short-term STAT3i treatment was applied. The same time points (30 min and 2 h) were tested with 5 and 10 µM concentrations of STAT3i, also based on previous results and the literature [69]. Considering the western blot analysis, the promising treatment chosen to reduce P-STAT3 protein levels was the STAT3i 5 µM for 2 hours (**Figure 3.5.2A, B**). Unexpectedly, the cells tested with STAT3i 5 µM in the following experiments did not survive. Therefore, further experiments are needed to fine tune the correct STAT3i concentrations for this analysis.

A.

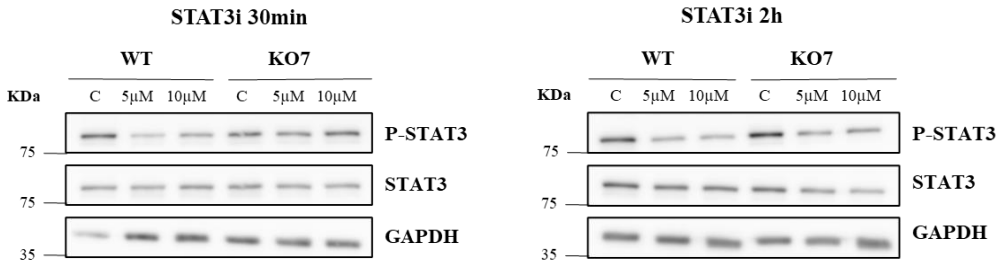

B.

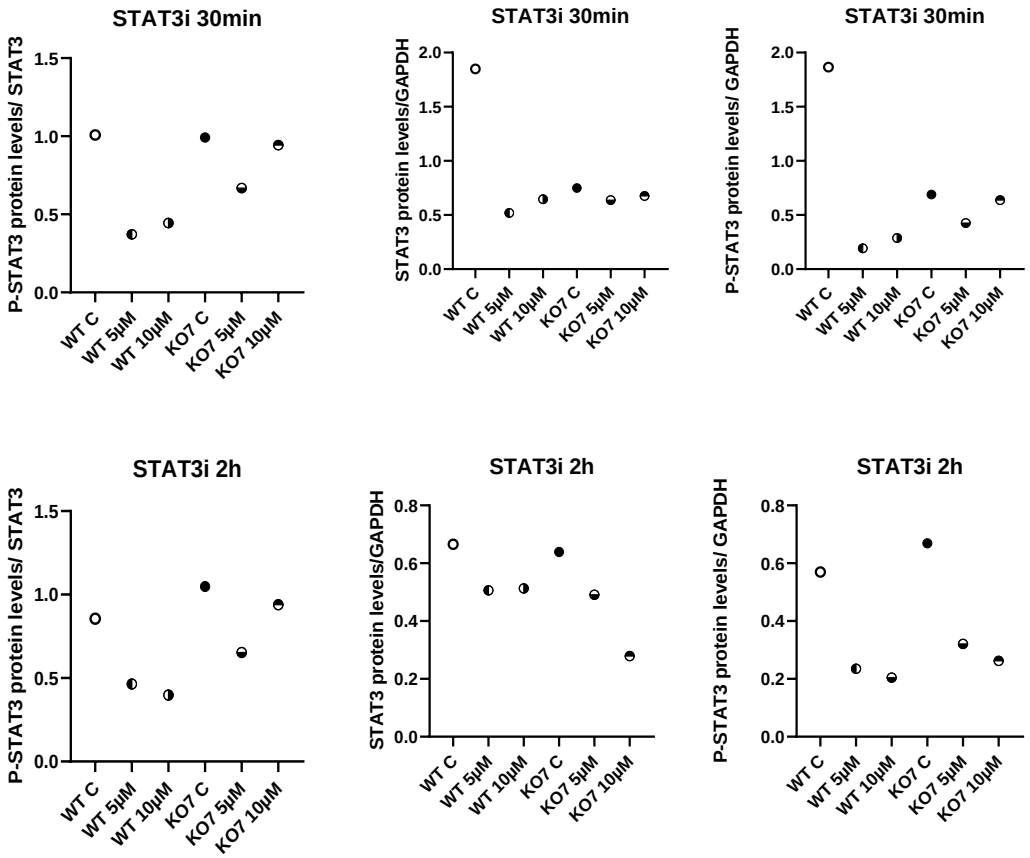

Figure 3.5.2 – Optimization of short-term STAT3 inhibitor treatment using WT and *Lama2* KO C2C12 cell lines. **A.** Representative western blot analysis of P-STAT3 Y705 (Tyrosine 705) in WT and one independent C2C12 *Lama2* single cell KO (KO7) treated with two different concentrations (5 and 10 µM) STAT3 inhibitor (STAT3i) (Stattic) in cell proliferation medium for 30 minutes (30 m) or 2 hours (2 h). GAPDH was used as loading control. **B.** Densitometry analysis of the western blot images in (A.). P-STAT3 protein levels from 30min and 2 h were normalized to STAT3 and GAPDH, n=1 experiment. C – control.

3.6. FAK, STAT3 and NFIX shRNA-mediated knockdown in WT and *Lama2* KO C2C12 cell lines

The absence of an effect of the inhibitor treatments on cell differentiation could be due to them being short-term. Next, the long-term effect was evaluated through silencing of some proteins, previously identified as overexpressed in *Lama2* KO C2C12 cell lines and/or *dyW* mouse model, using lentiviral infection of shRNA's targeting FAK, STAT3 and NFIX. For that, the transfection of the packaging cell

line HEK 293T was optimized by testing HBS buffers (HEPES buffered saline) with different pH, which is critical for calcium-phosphate precipitation during transfection. Of the tested pH, pH 7.05 apparently leads to fewer transfected cells while the others appear to be of equivalent efficiency (see **Figure S3** in annex). The pH 7.11 buffer solution was chosen for further experiments. The choice of shRNA sequences was taken from articles that show efficient target proteins reductions in mouse [39,70,71]. Before proceeding with lentiviral infections of WT and *Lama2* KO C2C12 cell lines, after cloning selected plasmids, were sequenced and the presence of shFAK, shSTAT3 and shNFIX was confirmed (see **Figure S4** in annex). The WT and two *Lama2* C2C12 KO cell lines (KO7 and KOE) were infected with lentivirus carrying recombinant pLKO.1 plasmids each expressing a specific shRNA targeting luciferase, FAK, STAT3 and NFIX proteins expression. Luciferase is an enzyme from fireflies responsible for light emission through an enzymatic oxidation reaction [72]. Since the C2C12 cells do not express luciferase, shRNA targeting luciferase is not expected to modify the expression of any gene and was, therefore, used as control. The protein silencing, after puromycin selection, was analyzed by western blot (**Figure 3.6A**). The densitometric analyze of respective western blots did not show reduction on target proteins in cells transfected with the different shRNA's (**Figure 3.6B**).

A.

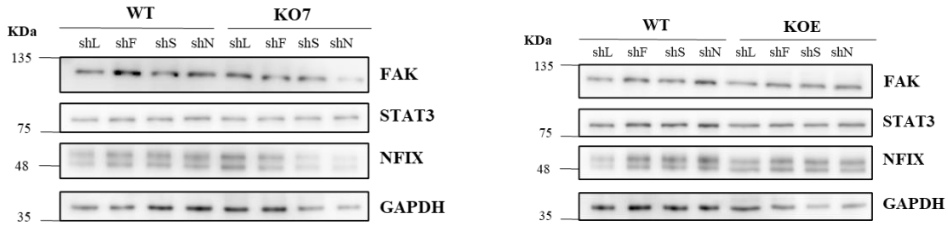

B.

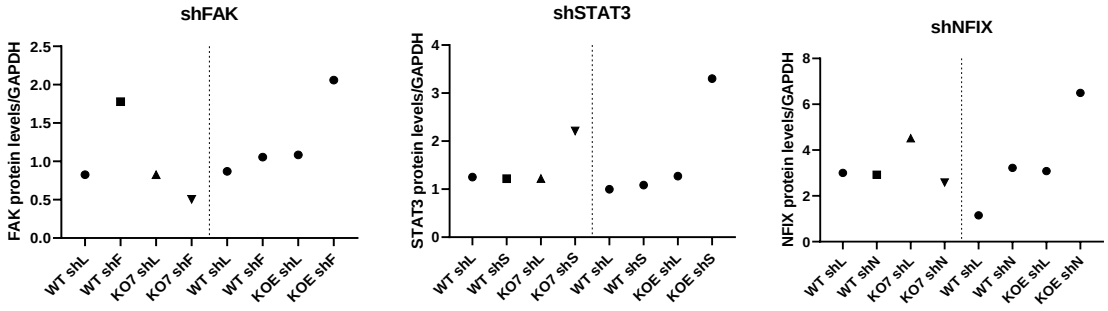

Figure 3.6 – Lentiviral infection using shRNA's targeting FAK, STAT3 and NFIX in WT and *Lama2* KO cell lines. **A.** Western blot analysis of FAK, STAT3 and NFIX in WT and two independent *Lama2* C2C12 single cell KO (KO7 and KOE). GAPDH was used as loading control. WT and two *Lama2* C2C12 KO cell lines (KO7 and KOE) were infected with lentivirus carrying shRNA Luciferase (shL), as control, shRNA FAK (shF), shRNA STAT3 (shSTAT3), or shRNA NFIX (shN), harvested after puromycin selection for 3 days. **B.** Densitometric analysis of western blot in (**A**). FAK, STAT3 and NFIX protein levels were normalized to GAPDH. The protein knockdown expression is compared to respective Luciferase plasmid transfection, n= 1 experiment.

4. Discussion

LAMA2-CMD is a genetic disease caused by mutations in the *LAMA2* gene that encode the laminin α2 chain present in laminins 211 and 221 [8,48]. Currently, there is no cure or targeted treatment for LAMA2-CMD. Available treatments are aimed at ameliorating some of the symptoms and involve a multidisciplinary medical team [48]. The use of animal mouse models has allowed a better understanding of the main mechanisms linked to the disease which will help to develop new therapeutic strategies [52]. Previous studies from the host laboratory showed that the absence of *Lama2* in *dyW* mouse model leads to the upregulation of some pathways in fetal muscle at E17.5, in particular STAT3 [55] and FAK (unpublished data).

The generation of *Lama2*-deficient KO cell lines, using CRISPR/Cas9 gene editing, is a well-established protocol (optimized by the host laboratory) that allows to further investigate which cellular and molecular mechanisms differ in the absence of *Lama2*. In this work, the transfection of the WT C2C12 cell lines with three plasmids was successful and four *Lama2* KO clones were established in less than 2 months (**Figure 3.1A, B**). Two of these KO clones (KO7 and KO8) were initially selected to proceed with characterization, though the *Lama2* KO8 cell line was eliminated from the analysis. Despite the low *Lama2* mRNA expression, which is suggestive of successful deletion, the KO8 clone had a different morphology and lower ability to be maintained *in vitro* compared to the other *Lama2* KO cell lines. This may be explained by the risk of off-target effects associated with Cas9 expression [73], as well as by cell-specific mutations that can occur during the clonal expansion of single cell clones. These reasons can also explain the variability observed when different clones were compared. Accordingly, all experiments were caried out using two *Lama2* KO cell lines that originated from different single cell clones, in order to guarantee that results obtained from this study are linked to the absence of *Lama2* gene and are not associated with the clonal specific phenotype. The sequence of the targeted genomic regions was analyzed and it was revealed that the exon 4 gRNA was efficient due to a nucleotide insertion responsible for changing the open reading frame. The exon 9 sequencing was difficult to analyze due to some extra peaks observed in all sequence (**Figure 3.1D**). The low efficiency related to exon 9 gRNA can be explained by it being a mouse target sequence that differs in one nucleotide compared with WT C2C12 exon 9 sequence (**Figure S1** in Annex). Therefore, the *Lama2* KO generation using CRISPR/Cas9 gene editing was successful and the selection of KO7, beyond the low *Lama2* expression, was based on the similar phenotype as the previously characterized clones. Some particular markers, such as P-STAT3 and HO-1, were also found to be overexpressed in this *Lama2*-deficient clone cell line showing that these cells experience oxidative stress (**Figure 3.1E, F**).

The differentiation of myoblast cells is a crucial step during myogenesis that culminates in the generation of muscle fibers [13]. Previous results from the host laboratory have shown a delay in myoblast differentiation in *Lama2* KO clones using differentiation media from day zero of culture. The differentiation media is supplemented with 2 % of horse serum, instead of the usual 10 % FBS. The 2 % of horse serum medium has fewer growth factors which promote the switch from proliferation state to differentiation state [74]. However, there was the possibility that the low serum levels in the medium could accentuate the proliferation defect of *Lama2* KO cells, thereby influencing the number of cells available to fuse and form myotubes. This might have been the cause for the differentiation defects observed. Consequently, cell differentiation was induced by high confluence in proliferation medium (with 10 % fetal bovine serum). Even though both WT and *Lama2* KO cells were allowed to achieve 100 % confluency, the same defect in the differentiation of *Lama2* KO cells was observed. This allowed to conclude that the observed impairment of myofiber formation in *Lama2* KO cells is a condition caused by the absence of the *Lama2* gene. In a similar study, the knockdown of a small ubiquitin-like modifier (SUMO)-conjugated enzyme, Ubc9, also identified defects in differentiation of C2C12 cells with a reduction in fibers formation [75]. Moreover, even though some *Lama2* KO cells were able to induce the

expression of myosin heavy chain, fusion of myoblasts to form multinucleated muscle fibers, was impaired and *Lama2* KO cells has fewer nuclei per fiber compared to the fibers formed by WT cells. In WT cells around 18 % of the myosin-positive cells have one nucleus per fiber and 19 % have more than four nuclei per fiber. The few myosin-positive cells observed in *Lama2* KO cells have mainly one nucleus (93%) and fibers with three or more nuclei were not observed (**Figure 3.2**). The differentiation defect of *Lama2* KO cells may have multiple causes. Previous results from the host laboratory suggested alterations in some TF directly related to muscle developmental, such as YAP, NFIX and MYF5. Since the function of TFs is to bind to DNA sequences and control the transcription of genes, their main activity is located in the nucleus [76]. A cell fractionation was conducted to assess the localization of these TFs in *Lama2* KO cells. It was previously observed by immunofluorescence that there was a tendency for a decrease in nuclear YAP in the *Lama2* KO cell lines when compared to WT (unpublished data). After several cell fractionation trials and western blot analyses, the difficulty of locating YAP remains, as different bands sizes were observed in both nuclear and cytoplasmic fractions (**Figure 3.3A**). These discrepant band sizes maybe related to posttranslational modifications, particularly with different phosphorylation, when cells were harvested[46]. It is known that YAP localization (nuclear or cytoplasmic) depends on its activation and the type of phosphorylation. YAP phosphorylation on Ser127 sequesters YAP in the cytoplasm (inactivated YAP), where it is unable to stimulate the expression of target genes. In contrast, the unphosphorylated YAP translocate to the nucleus (activated YAP) to induce the expression of target genes such as CYR61, CTGF, AREG, MYC, Gli2, Vimentin and AXL [77]. In other words, YAP activation induces cell growth and proliferation, while YAP phosphorylation tends to cause cell cycle exit to undergo differentiation. Cell density was also reported to have a positive impact on cell differentiation [43,45]. Therefore, there are many external factors that influence YAP activity that might explain the difficulty to identify YAP signaling in the *Lama2* KO cells. In future trials, it is necessary to consider the confluency at the exact moment that the cells are harvested. A more careful analysis will help to understand whether *Lama2* deletion alters YAP localization and whether it contributes to the proliferation and differentiation defects found in these cells. Supporting the important role of YAP during myogenesis, the YAP interaction partner, TEAD, was found to be essential to activate *Myf5* expression [18]. This raises the possibility that the lower expression of MYF5 observed in the nuclei, as well as the tendency for a reduction in MYF5 cytoplasmic levels in *Lama2* KO cells, may be related to lower YAP activity. MYF5 plays a major role in the onset of embryonic myogenesis via the regulation of multiple enhancers. Other TFs involved in the regulation of *Myf5* transcription are the *Six* genes (Since oculis homeobox genes 1 to 6) that are expressed during embryonic stages [78]. Considering the strong reduction of MYF5 localization in the nucleus of *Lama2*-deficient cells, it is possible that might be retained in the cytoplasm [59] (**Figure 3.3**), though why this would occur is still unknown. The study of the *Six* genes, more specifically the *Six1* and *Six4* [78], in *Lama2*-deficient cells could address whether they contribute to the translocation of MYF5 into the nucleus in these cell lines. Previous data from the laboratory [59] also showed an increase in the levels of NFIX in *Lama2* KO cells. NFIX acts as transcriptional activator or repressor and is mainly expressed in the fetus as marker of the embryonic-to-fetal transcriptional switch in skeletal muscle [23]. Adding to the previous findings, this work showed that NFIX was significantly increased in both nuclear and cytoplasmic fractions in *Lama2*-deficient cells. In the absence of *Lama2*, NFIX is upregulated (**Figure 3.3**). For this reason, it would be expected that this upregulation leads to myofibers formation. However, the observed results reveal that few myofibers form in *Lama2*-deficient cells and the ones present are aberrant (**Figure 3.2A, B**). Therefore, it is possible that the NFIX pathway is compromised. There is some evidence that NFIX exacerbates oxidative stress triggered by the presence of damaged fibers [24]. A recent study reported that in a dystrophic *Nfix* null mouse model the cycles of regeneration and degeneration were stabilized, while there was a reduction in oxidative stress linked to the switch towards oxidative slow-twitch fibers [25]. Based on this, an shRNA approach was tested to silence NFIX, though some issues related to the

pLKO.1 plasmid precluded the reduction of NFIX levels *in vitro* (**Figure 3.6**) and whether NFIX downregulation could revert the *Lama2* KO phenotype.

As previously mentioned, some pathways were identified as being upregulated, including FAK and JAK/STAT pathways responsible for cell adhesion, proliferation, and differentiation, among other features. In an attempt to rescue the *Lama2* KO phenotype, pharmacological inhibitors were used to inhibit the active proteins. As first trials of inhibitor titrations, the cells were incubated for 3 days with several concentrations to access the long-term effects, which would be important to determine, for example, their impact on myoblast differentiation. The ideal concentration of inhibitors was not found in these conditions, most likely due to the long duration of the treatment and the difficulty to adjust the dose (**Figures 3.4.1 and 3.5.1**). The way to counter this issue was to reduce the duration of the treatment with the inhibitors (30 min and 2 h) and analyze short-term effects, such as oxidative stress. As this phenotype is characteristic of the *Lama2*-deficient cells, immediate effects were expected to be observed. After finding the ideal concentration that reduce the levels of P-FAK in all cell lines (FAKi 3 μM for 2 h), a tendency for a decrease in P-STAT3 levels was also observed for the WT cells, which suggested that STAT3 signaling could be downstream of FAK pathway [41] (**Figure 3.4.2**). However, additional experiments need to be done to confirm this hypothesis. And other FAKi should also be tested so that we can properly normalize P-FAK levels to FAK. Under the above mentioned conditions, no reduction was observed in the oxidative stress marker HO-1, in short-term FAKi treatments, suggesting that the oxidative stress in *Lama2*-deficient cells is not downstream of the FAK pathway. Moreover, when the NFIX was analyzed after FAKi treatment no reduction was observed (**Figure 3.4.3I, J**). The hypothesis that overactivation of FAK leads to oxidative stress and, consequently, increased NFIX expression needs to be better explored with long-term FAKi treatments. Additionally, it was also tested if the inhibition of FAK would improve myofiber formation, though no change was observed in *Lama2 KO* cells (**Figure 3.4.4**). This suggests once again that the short-term FAKi treatment is not sufficient to target issues related to the differentiation process. Other evidence that has emerged with FAKi treatments is that it also affects vinculin levels as can be observed in **Figure 3.4.1D**. Vinculin is commonly used as a loading control due its constitutive expression in cells. This protein is present in cytoplasm and interacts with integrins to cell-matrix adhesions or focal adhesions, as well as cell-cell adhesions or adherent junctions [65]. When the FAK pathway is activated, integrin tails associate with vinculin and the actin binding protein, talin, which lead to focal adhesion activation [79]. This may explain the alterations in vinculin levels with FAKi treatments. Total FAK is also altered with FAKi treatments without clear explanation since the inhibitor acts at the phosphorylation level. Is also possible that the FAKi is not entirely specific, which would explain some of these findings. Given the same problems associated with the long-term effects of FAKi treatments, the same short-term strategy was applied to STAT3i treatments (**Figure 3.5.2**). After choosing the ideal concentration, the cells did not survive in culture in the following experiments for unknown reasons. To improve this, is important to be careful with cell toxicity and test with the lowest concentration as a potentially viable solution.

Considering the issues associated with the use of pharmacologic inhibitors and also as a complementary strategy, gene silencing of FAK and STAT3 shRNA was tested as an alternative approach to assess the long-term effects, while avoiding the cell toxicity caused by the inhibitors. To do so, a lentiviral infection protocol was used. The lentiviral ability to transduce dividing and non-dividing cells increases the efficiency of the plasmid delivery, making it an extremely useful protocol to test a knockdown [62]. Despite this, no reduction in target proteins was observed (**Figure 3.6**). The shRNA sequences were obtained from other papers using C2C12 cells [39,70] and a mouse model [71]. The plasmid shRNA sequence insert was validated by Sanger Sequencing (**Figure S4** in annex). One possibility is that the problem is associated with the pLKO.1 plasmid backbone. Many cycles of freezing and thawing can lead to introducing point mutations and degradation of the plasmid that prevents its correct functioning. As an alternative, a new infection with a new plasmid needs to be done and, if the problem

persists, a new strategy needs to be applied, such as a CRISPR interference lentiviral vector (dCas9-KRAB). This system is based on the fusion of inactive Cas9 (dCas9) to the Krüppel-associated box (KRAB) repressor domain to silencing the gene expression [80].

Altogether, the results obtained in this project intensify the idea that FAK pathway links to the STAT3 pathway and also confirm the nuclear overactivation of NFIX in *Lama2*-deficient cells. Additionally, this work also raised new questions, such as whether promoting activation of YAP in *Lama2*-deficient cells can increase the MYF5 levels. With the long-term FAK, STAT3 and NFIX inhibition analysis, it is expected that the *Lama2*-deficient cells recover proliferation capacity, undergo differentiation, and improve the oxidative stress levels. Therefore, FAK inhibition could be the key to recover some central aspects of the LAMA2-CMD phenotype. After testing this *in vitro*, the next step would be to test this inhibition in the *dyW* mouse model with gene silencing therapy. Since gene therapy directed to the *LAMA2* gene is conditioned to the type of mutation, which is variable, acting on targets activated by the interaction of cells to laminins, may be an alternative strategy to develop new therapies for this incurable and often lethal disease.

5. References

1. Frantz, C., Stewart, K. M. & Weaver, V. M. The extracellular matrix at a glance. *Journal of Cell Science* vol. 123 4195–4200 Available from: https://doi.org/10.1242/jcs.023820 (2010).
2. Yue, B. Biology of the extracellular matrix: An overview. *Journal of Glaucoma* vol. 23 S20–S23 Available from: https://doi.org/10.1097/IJG.0000000000000108 (2014).
3. Mouw, J. K., Ou, G. & Weaver, V. M. Extracellular matrix assembly: A multiscale deconstruction. *Nature Reviews Molecular Cell Biology* vol. 15 771–785 Available from: https://doi.org/10.1038/nrm3902 (2014).
4. Hamill, K. J., Kligys, K., Hopkinson, S. B. & Jones, J. C. R. Laminin deposition in the extracellular matrix: A complex picture emerges. *J Cell Sci* **122**, 4409–4417 (2009).
5. Ishihara, J. *et al.* Laminin heparin-binding peptides bind to several growth factors and enhance diabetic wound healing. *Nat Commun* **9**, (2018).
6. Boppart, M. D. & Mahmassani, Z. S. THEME New and Emerging Roles of the Cytoskeleton in Striated Muscle Integrin signaling: linking mechanical stimulation to skeletal muscle hypertrophy. *Am J Physiol Cell Physiol* **317**, 629–641 (2019).
7. Israeli-Rosenberg, S., Manso, A. M., Okada, H. & Ross, R. S. Integrins and integrin-associated proteins in the cardiac myocyte. *Circulation Research* vol. 114 572–586 Available from: https://doi.org/10.1161/CIRCRESAHA.114.301275 (2014).
8. About MDC1A - LAMA2. https://lama2.com/about-mdc1a/.
9. Barraza-Flores, P., Bates, C. R., Oliveira-Santos, A. & Burkin, D. J. Laminin and Integrin in LAMA2-Related Congenital Muscular Dystrophy: From Disease to Therapeutics. *Frontiers in Molecular Neuroscience* vol. 13 Available from: https://doi.org/10.3389/fnmol.2020.00001 (2020).
10. Holmberg, J. & Durbeej, M. Laminin-211 in skeletal muscle function. *Cell Adhesion and Migration* vol. 7 111–121 Available from: https://doi.org/10.4161/cam.22618 (2013).
11. Braithwaite JP, Al Khalili Y. Physiology, Muscle Myocyte. [Updated 2023 May 1]. In: StatPearls [Internet]. Treasure Island (FL): StatPearls Publishing; 2023 Jan-. Available from: https://www.ncbi.nlm.nih.gov/books/NBK544225/
12. Dave HD, Shook M, Varacallo M. Anatomy, Skeletal Muscle. [Updated 2022 Aug 30]. In: StatPearls [Internet]. Treasure Island (FL): StatPearls Publishing; 2023 Jan-. Available from: https://www.ncbi.nlm.nih.gov/books/NBK537236/

13. Fiorotto M. (2012). The making of a muscle. The biochemist, 34(3), 4–11.
14. Buckingham, M. & Relaix, F. PAX3 and PAX7 as upstream regulators of myogenesis. *Seminars in Cell and Developmental Biology* vol. 44 115–125 Available from: https://doi.org/10.1016/j.semcdb.2015.09.017 (2015).
15. Bentzinger, C. F., Wang, Y. X. & Rudnicki, M. A. Building muscle: molecular regulation of myogenesis. *Cold Spring Harbor perspectives in biology* vol. 4 Available from: https://doi.org/10.1101/cshperspect.a008342 (2012).
16. Zammit, P. S. Function of the myogenic regulatory factors Myf5, MyoD, Myogenin and MRF4 in skeletal muscle, satellite cells and regenerative myogenesis. *Seminars in Cell and Developmental Biology* vol. 72 19–32 Available from: https://doi.org/10.1016/j.semcdb.2017.11.011 (2017).
17. Francetic, T. & Li, Q. Skeletal myogenesis and Myf5 activation. *Transcription* **2**, 109–114 (2011).
18. Ribas, R. *et al.* Members of the TEAD family of transcription factors regulate the expression of Myf5 in ventral somitic compartments. *Dev Biol* **355**, 372–380 (2011).
19. Yoshimoto, Y., Ikemoto-Uezumi, M., Hitachi, K., Fukada, S. I. & Uezumi, A. Methods for Accurate Assessment of Myofiber Maturity During Skeletal Muscle Regeneration. *Front Cell Dev Biol* **8**, (2020).
20. Asfour, H. A., Allouh, M. Z. & Said, R. S. Myogenic regulatory factors: The orchestrators of myogenesis after 30 years of discovery. *Exp Biol Med* **243**, 118–128 (2018).
21. Millay, D. P. Regulation of the myoblast fusion reaction for muscle development, regeneration, and adaptations. *Exp Cell Res* **415**, (2022).
22. Messina, G. *et al.* Nfix Regulates Fetal-Specific Transcription in Developing Skeletal Muscle. *Cell* **140**, 554–566 (2010).
23. Rossi, G. *et al.* Nfix Regulates Temporal Progression of Muscle Regeneration through Modulation of Myostatin Expression. *Cell Rep* **14**, 2238–2249 (2016).
24. Ribeiro, V. *et al.* NFIXing Cancer: The Role of NFIX in Oxidative Stress Response and Cell Fate. *International Journal of Molecular Sciences* vol. 24 Available from: https://doi.org/10.3390/ijms24054293 (2023).
25. Rossi, G. *et al.* Silencing Nfix rescues muscular dystrophy by delaying muscle regeneration. *Nat Commun* **8**, (2017).
26. Margadant, C., Monsuur, H. N., Norman, J. C. & Sonnenberg, A. Mechanisms of integrin activation and trafficking. *Current Opinion in Cell Biology* vol. 23 607–614 Available from: https://doi.org/10.1016/j.ceb.2011.08.005 (2011).
27. Bauer, M. S. *et al.* Structural and mechanistic insights into mechanoactivation of focal adhesion kinase. *Proc Natl Acad Sci U S A* **116**, 6766–6774 (2019).
28. Graham, Z. A., Gallagher, P. M. & Cardozo, C. P. Focal adhesion kinase and its role in skeletal muscle. *Journal of Muscle Research and Cell Motility* vol. 36 305–315 Available from: https://doi.org/10.1007/s10974-015-9415-3 (2015).
29. Slack-Davis, J. K. *et al.* Cellular characterization of a novel focal adhesion kinase inhibitor. *Journal of Biological Chemistry* **282**, 14845–14852 (2007).
30. Murphy, J. M., Park, H. & Lim, S. T. S. FAK and Pyk2 in disease. *Front Biol (Beijing)* **11**, 1–9 (2016).
31. Frame, M. C., Patel, H., Serrels, B., Lietha, D. & Eck, M. J. The FERM domain: Organizing the structure and function of FAK. *Nature Reviews Molecular Cell Biology* vol. 11 802–814 Available from: https://doi.org/10.1038/nrm2996 (2010).

32. Zhou, J., Yi, Q. & Tang, L. The roles of nuclear focal adhesion kinase (FAK) on Cancer: A focused review. *Journal of Experimental and Clinical Cancer Research* vol. 38 Available from: https://doi.org/10.1186/s13046-019-1265-1 (2019).
33. Luo, S. W. *et al.* Regulation of heterochromatin remodelling and myogenin expression during muscle differentiation by FAK interaction with MBD2. *EMBO Journal* **28**, 2568–2582 (2009).
34. Li, J., Yin, Z., Huang, B., Xu, K. & Su, J. Stat3 Signaling Pathway: A Future Therapeutic Target for Bone-Related Diseases. *Frontiers in Pharmacology* vol. 13 Available from: https://doi.org/10.3389/fphar.2022.897539 (2022).
35. Wang, K., Wang, C., Xiao, F., Wang, H. & Wu, Z. JAK2/STAT2/STAT3 are required for myogenic differentiation. *Journal of Biological Chemistry* **283**, 34029–34036 (2008).
36. Tanaka, T., Narazaki, M. & Kishimoto, T. Il-6 in inflammation, Immunity, And disease. *Cold Spring Harb Perspect Biol* **6**, (2014).
37. Guadagnin, E., Mázala, D. & Chen, Y. W. STAT3 in skeletal muscle function and disorders. *International Journal of Molecular Sciences* vol. 19 Available from: https://doi.org/10.3390/ijms19082265 (2018).
38. Moresi, V., Adamo, S. & Berghella, L. The JAK/STAT pathway in skeletal muscle pathophysiology. *Frontiers in Physiology* vol. 10 Available from: https://doi.org/10.3389/fphys.2019.00500 (2019).
39. Sun, L. *et al.* JAK1-STAT1-STAT3, a key pathway promoting proliferation and preventing premature differentiation of myoblasts. *Journal of Cell Biology* **179**, 129–138 (2007).
40. Hsu, P. C., Yang, C. T., Jablons, D. M. & You, L. The crosstalk between src and hippo/YAP signaling pathways in non-small cell lung cancer (NSCLC). *Cancers* vol. 12 Available from: https://doi.org/10.3390/cancers12061361 (2020).
41. Portillo, J. A. C. *et al.* Toxoplasma gondii induces FAK-Src-STAT3 signaling during infection of host cells that prevents parasite targeting by autophagy. *PLoS Pathog* **13**, (2017).
42. Lachowski, D. *et al.* FAK controls the mechanical activation of YAP, a transcriptional regulator required for durotaxis. *FASEB Journal* **32**, 1099–1107 (2018).
43. Heng, B. C. *et al.* Role of YAP/TAZ in Cell Lineage Fate Determination and Related Signaling Pathways. *Frontiers in Cell and Developmental Biology* vol. 8 Available from: https://doi.org/10.3389/fcell.2020.00735 (2020).
44. Owens, D. J. *et al.* Lamin Mutations Cause Increased YAP Nuclear Entry in Muscle Stem Cells. *Cells* **9**, (2020).
45. Fu, M. *et al.* The Hippo signalling pathway and its implications in human health and diseases. *Signal Transduction and Targeted Therapy* vol. 7 Available from: https://doi.org/10.1038/s41392-022-01191-9 (2022).
46. Kastan, N. *et al.* Small-molecule inhibition of Lats kinases may promote Yap-dependent proliferation in postmitotic mammalian tissues. *Nat Commun* **12**, (2021).
47. Watt, K. I. *et al.* The Hippo pathway effector YAP is a critical regulator of skeletal muscle fibre size. *Nat Commun* **6**, (2015).
48. Oliveira, J. *LAMA2 Muscular Dystrophy-GeneReviews Phenotypic variability and modifier genes in Familial Amyloid Polyneuropathy (FAP ATTRV30M) View project*. https://www.ncbi.nlm.nih.gov/books/ (1993).
49. Hashemi-Gorji, F., Yassaee, V. R., Dashti, P. & Miryounesi, M. Novel LAMA2 gene mutations associated with merosin-deficient congenital muscular dystrophy. *Iran Biomed J* **22**, 408–414 (2018).
50. Oliveira, J. *et al.* LAMA2 gene mutation update: Toward a more comprehensive picture of the laminin-α2 variome and its related phenotypes. *Hum Mutat* **39**, 1314–1337 (2018).

51. Accorsi, A., Cramer, M. L. & Girgenrath, M. Fibrogenesis in LAMA2-Related Muscular Dystrophy Is a Central Tenet of Disease Etiology. *Frontiers in Molecular Neuroscience* vol. 13 Available from: https://doi.org/10.3389/fnmol.2020.00003 (2020).
52. Gawlik, K. I. & Durbeej, M. A Family of Laminin α2 Chain-Deficient Mouse Mutants: Advancing the Research on LAMA2-CMD. *Frontiers in Molecular Neuroscience* vol. 13 Available from: https://doi.org/10.3389/fnmol.2020.00059 (2020).
53. Pasteuning-Vuhman, S. *et al.* Natural disease history of the dy2J mouse model of laminin α2 (merosin)-deficient congenital muscular dystrophy. *PLoS One* **13**, (2018).
54. Willmann, R. *et al.* Improving Reproducibility of Phenotypic Assessments in the DyW Mouse Model of Laminin-α2 Related Congenital Muscular Dystrophy. *Journal of Neuromuscular Diseases* vol. 4 115–126 Available from: https://doi.org/10.3233/JND-170217 (2017).
55. Nunes, A. M. *et al.* Impaired fetal muscle development and JAK-STAT activation mark disease onset and progression in a mouse model for merosin-deficient congenital muscular dystrophy. *Hum Mol Genet* **26**, 2018–2033 (2017).
56. Gawlik, K. I., Körner, Z., Oliveira, B. M. & Durbeej, M. Early skeletal muscle pathology and disease progress in the dy 3K /dy 3K mouse model of congenital muscular dystrophy with laminin α2 chain-deficiency. *Sci Rep* **9**, (2019).
57. Barraza-Flores, P. *et al.* Human laminin-111 and laminin-211 protein therapy prevents muscle disease progression in an immunodeficient mouse model of LAMA2-CMD. *Skelet Muscle* **10**, (2020).
58. Kemaladewi, D. U. *et al.* A mutation-independent approach for muscular dystrophy via upregulation of a modifier gene. *Nature* **572**, 125–130 (2019).
59. Ribeiro, V. F. L. How Lama2-deficiency impacts myoblast differentiation in a mouse model for LAMA2-congenital muscular dystrophy. *Repositório da Universidade de Lisboa* Available from: https://repositorio.ul.pt/handle/10451/55503 (2022).
60. Yaffe, D. & Saxel, O. Serial passaging and differentiation of myogenic cells isolated from dystrophic mouse muscle. *Nature 1977 270:5639* **270**, 725–727 (1977).
61. Xu, J. *et al.* Construction of Conveniently Screening pLKO.1-TRC Vector Tagged with TurboGFP. *Appl Biochem Biotechnol* **181**, 699–709 (2017).
62. Poletti, V. & Mavilio, F. Designing lentiviral vectors for gene therapy of genetic diseases. *Viruses* vol. 13 Available from: https://doi.org/10.3390/V13081526 (2021).
63. Melo, C. E. M. de & Carlos, A. R. C. M. The impact of Lama2-deficiency on cell cycle regulation and survival. *Repositório da Universidade de Lisboa* Available from: https://repositorio.ul.pt/handle/10451/53636 (2022).
64. Vollert, C. S. & Uetz, P. Comparative Proteomes of the Proliferating C2C12 Myoblasts and Fully Differentiated Myotubes Reveal the Complexity of the Skeletal Muscle Differentiation Program. *Molecular and Cellular Proteomics* **3**, 1053–1064 (2004).
65. Peng, X., Nelson, E. S., Maiers, J. L. & DeMali, K. A. New Insights into Vinculin Function and Regulation. in *International Review of Cell and Molecular Biology* vol. 287 191–231 (Elsevier Inc., 2011).
66. Bhasin, M., Reinherz, E. L. & Reche, P. A. Recognition and classification of histones using support vector machine. *Journal of Computational Biology* **13**, 102–112 (2006).
67. Nana, F. A. *et al.* Therapeutic potential of focal adhesion kinase inhibition in small cell lung cancer. *Mol Cancer Ther* **18**, 17–27 (2019).
68. Guo, H. *et al.* Inhibition of STAT3Y705 phosphorylation by Stattic suppresses proliferation and induces mitochondrial-dependent apoptosis in pancreatic cancer cells. *Cell Death Discov* **8**, (2022).

69. Schust, J., Sperl, B., Hollis, A., Mayer, T. U. & Berg, T. Stattic: A Small-Molecule Inhibitor of STAT3 Activation and Dimerization. *Chem Biol* **13**, 1235–1242 (2006).
70. Crossland, H. *et al.* Focal adhesion kinase is required for IGF-I-mediated growth of skeletal muscle cells via a TSC2/mTOR/S6K1-associated pathway. *Am J Physiol Endocrinol Metab* **305**, 183–193 (2013).
71. Holmfeldt, P. *et al.* Nfix is a novel regulator of murine hematopoietic stem and progenitor cell survival Key Points. (2013) doi:10.1182/blood-2013.
72. Khakhar, A. *et al.* Building customizable auto-luminescent luciferase-based reporters in plants. *Elife* **9**, (2020).
73. Guo, C., Ma, X., Gao, F. & Guo, Y. Off-target effects in CRISPR/Cas9 gene editing. *Frontiers in Bioengineering and Biotechnology* vol. 11 Available from: https://doi.org/10.3389/fbioe.2023.1143157 (2023).
74. Pirkmajer, S. & Chibalin, A. V. Serum starvation: caveat emptor. *J Physiol Cell Physiol* **301**, 272–279 (2011).
75. Riquelme, C., Barthel, K. K. B., Qin, X. F. & Liu, X. Ubc9 expression is essential for myotube formation in C2C12. *Exp Cell Res* **312**, 2132–2141 (2006).
76. Mitsis, T. *et al.* Transcription factors and evolution: An integral part of gene expression (Review). *World Academy of Sciences Journal* vol. 2 3–8 Available from: https://doi.org/10.3892/wasj.2020.32 (2020).
77. Kim, M. K., Jang, J. W. & Bae, S. C. DNA binding partners of YAP/TAZ. *BMB Reports* vol. 51 126–133 Available from: https://doi.org/10.5483/BMBRep.2018.51.3.015 (2018).
78. Giordani, J. *et al. Six proteins regulate the activation of Myf5 expression in embryonic mouse limbs*. www.pnas.org/cgi/content/full/ (2007).
79. Pasapera, A. M., Schneider, I. C., Rericha, E., Schlaepfer, D. D. & Waterman, C. M. Myosin II activity regulates vinculin recruitment to focal adhesions through FAK-mediated paxillin phosphorylation. *Journal of Cell Biology* **188**, 877–890 (2010).
80. Alerasool, N., Segal, D., Lee, H. & Taipale, M. An efficient KRAB domain for CRISPRi applications in human cells. *Nat Methods* **17**, 1093–1096 (2020).

6. Annex

Table S1 - List of antibodies used in western blot and immunofluorescence

ANTIBODY	RAISED IN	PRIMARY/ SECONDARY	DILUTION	CATALOG NUMBER	BRAND
WESTERN BLOT					
P-FAK Y397	Rabbit	Primary	1:1000	PA5-17084	Invitrogen
FAK	Mouse	Primary	1:1000	sc-1688	Santa Cruz
P-STAT3 Y705	Rabbit	Primary	1:1000	9145	Cell Signaling
STAT3	Rabbit	Primary	1:1000	12640	Cell Signaling
YAP	Rabbit	Primary	1:1000	4912	Cell Signaling
MYF5	Mouse	Primary	1:1000	Ma5-26654	Invitrogen
NFIX	Rabbit	Primary	1:1000	nbp2-415039	Novus Biologicals
HISTONE H3	Rabbit	Primary	1:2000	9715	Cell Signaling
HO-1	Rabbit	Primary	1:1000	SPA-896	Enzo Life Sciences
GAPDH	Rabbit	Primary	1:2000	2118	Cell Signaling
VINCULIN	Mouse	Primary	1:2000	ab18058	Abcam
ANTI-MOUSE HRP	Goat	Secondary	1:5000	NA931	GE Healthcare
ANTI-RABBIT	Goat	Secondary	1:5000	NA934	GE Healthcare
IMMUNOFLUORESCENCE					
MYOSIN	Mouse	Primary	1:200	MF-20	DSHB
ALEXA FLUOR 568 ANTI-MOUSE IGG	Goat	Secondary	1:500	A11019	Invitrogen

Table S2 - List of primers, gRNA, and shRNA sequences

GENE	SPECIES	OLIGO TYPE	SEQUENCE	REFERENCES
Lama2	Mouse	Forward primer	5' TGAAAGCAAGGCCAGAAGTCA 3'	This project
		Reverse primer	5' ACAAAACCAGGCTTGGGGAA 3'	This project
Arbp0/ Rplp0	Mouse	Forward primer	5' CTTTGGGCATCACCACGAA 3'	This project
		Reverse primer	5' GCTGGCTCCCACCTTGTCT 3'	This project
Tubb6	Mouse	Forward primer	5' AAGAAGTACGTACCCAGGGC 3'	This project
		Reverse primer	5' CACCCGTCTGTCCGAAGAT 3'	This project
Myl1	Mouse	Forward primer	5' CGGAGTTTTCAAGCACGCAA 3'	This project
		Reverse primer	5' TCTGCATGGTGGTAAGCTGG 3'	This project
Myog	Mouse	Forward primer	5' GTCCCAACCCAGGAGATCAT 3'	This project
		Reverse primer	5' CCACGATGGACGTAAGGGAG 3'	This project
Exon 4	Mouse	Forward primer	5' GTTTGCACTAATGCTGGACCC 3'	This project
Exon 9	Mouse	Reverse primer	5' TGAAGCCCACTGTGACATTTCT 3'	This project
U6	Mouse	Primer sequencing	5' AGTACAAAATACGTGACGTAG 3'	This project
gRNA *Lama2* Exon 4	Mouse	gRNA	5' GGCTGCCTTCACAATTACGT 3'	VectorBuilder
gRNA *Lama2* Exon 9	Mouse	gRNA	5' GATGAGAAATATGCCCAGCG 3'	VectorBuilder
shRNA FAK	Mouse	Forward shRNA	5'CCGGCAACCTTAATAGAGAAGAAACTCG AGTTTCTTCTCTATTAAGGTTGTTTTTG 3'	IDT DNA
		Reverse shRNA	5'AATTCAAAAACAACCTTAATAGAGAAGA AACTCGAGTTTCTTCTCTATTAAGGTTG 3'	IDT DNA
shRNA STAT3	Mouse	Forward shRNA	5'CCGGCTGGATAACTTCATTAGCACTCGAG TGCTAATGAAGTTATCCAGTTTTTG 3'	IDT DNA
		Reverse shRNA	5'AATTCAAAAACTGGATAACTTCATTAGCA CTCGAGTGCTAATGAAGTTATCCAG 3'	IDT DNA
shRNA NFIX	Mouse	Forward shRNA	5'CCGGCACATTGGAGTCACAATCAAACTCG AGTTTGATTGTGACTCCAATGTGTTTTTG 3'	IDT DNA
		Reverse shRNA	5'AATTCAAAAACACATTGGAGTCACAATCA AACTCGAGTTTGATTGTGACTCCAATGTG 3'	IDT DNA

Table S3 - Real time qPCR program used in CFX96™

REAL-TIME PCR SYSTEM		**BIO-RAD CFX96™**
SETTING/MODE		SYBR only
AMPLIFICATION	Polymerase Activation and DNA Denaturation	30 sec at 95 ºC
	Denaturation at 95 ºC	5 sec
	Annealing/Extension and Plate Read at 60 ºC	15 sec
CYCLES		40
MELTING CURVE ANALYSIS		65-95 ºC 0.5 ºC increments at 5 sec/step

Table S4 - 2x HSB Buffer from lentiviral infection protocol

SOLUTION	**FINAL CONCENTRATION**	**QUANTITY OF STOCK**
NaCl	0.28 M	16,4 g
HEPES (NO Na SALT)	50 mM	11,9 g
Na_2HPO_4	1.5 mM	0,21 g
STERIL WATER	In water	To 1 L
NaOH	pH 7.00 – 7.15	

Note - Were tested 4 different pH concentrations (pH 7.05, pH 7.08, pH 7.11 and pH 7.15) and the best concentration (pH 7.11) was stored at -20 ºC.

Table S5 - Reagents of Buffer A in cell fractionation protocol

SOLUTION	FINAL CONCENTRATION	ML OF STOCK (CONCENTRATION)
HEPES PH 7.9	10 mM	1 mL (0.5 M)
KCl	10 mM	500 µL (1 M)
$MgCl_2$	1.5 mM	75 µL (1 M)
SUCROSE	0.34 M	17 mL (1 M)
GLYCEROL	10 %	10 mL (50 %)
STERIL WATER	In water	50 mL

Table S6 - Lentiviral infection protocol reagents

PLASMID	CONTAINS	GENERATION	TYPE	REFERENCES
PRSV-REV	Rev	3rd	Packaging	Addgene#12253
PMDLG/PRRE	Gag and Pol	3rd	Packaging	Addgene#12251
PMD2.G	VSV-G	N/A	Envelope	Addgene#12259
pLKO.1 PURO	U6- driven shRNA empty plasmid with puromycin resistance cassette	3rd	Backbone	Addgene#8453

N/A – Not applicable

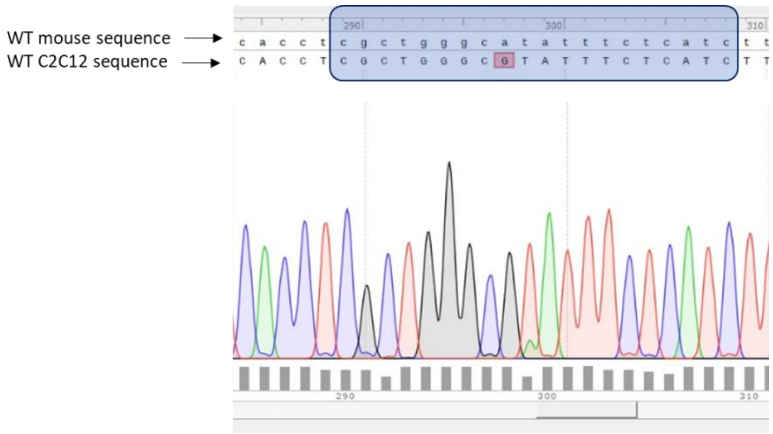

Figure S1 – WT mouse muscle and WT C2C12 cell sequence alignment. Sanger sequence alignment between muscle and cell WT amplified with exon9_Rev primer. Blue square indicate the exon9 gRNA sequence and the red square indicate the mismatch point between WT mouse and WT C2C12 sequence. The alignment and the analysis of the Sanger data were performed using the SnapGene software.

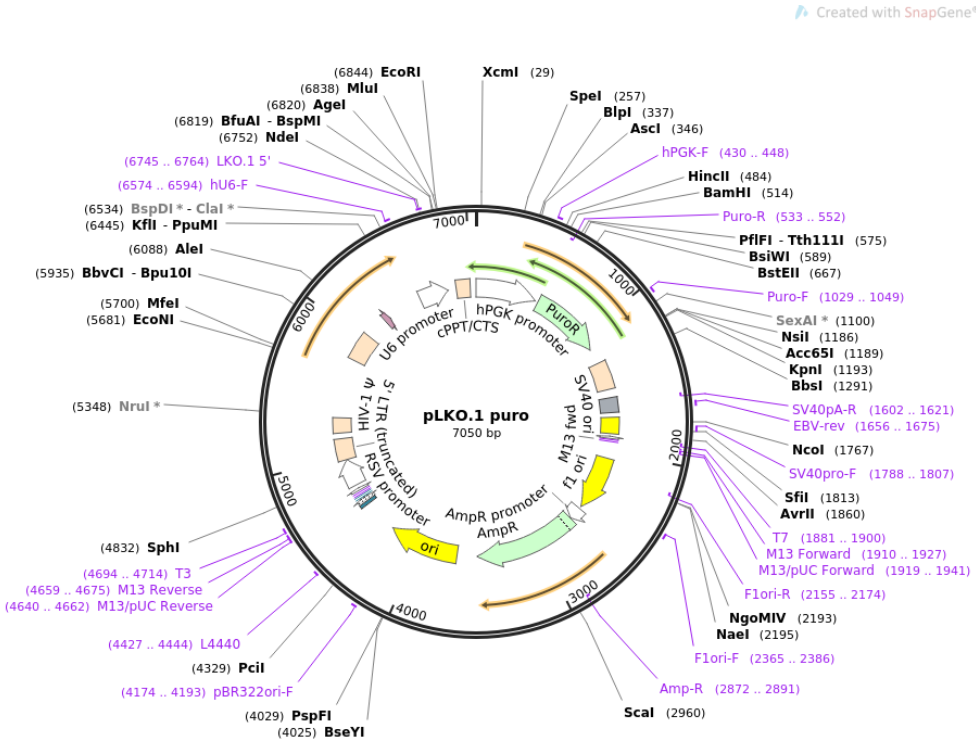

Figure S2 – Design of pLKO.1 puro. Map of empty 3rd generation vector backbone pLKO.1 used in lentiviral cloning with puromycin resistance. Image acquired from addgene.org.

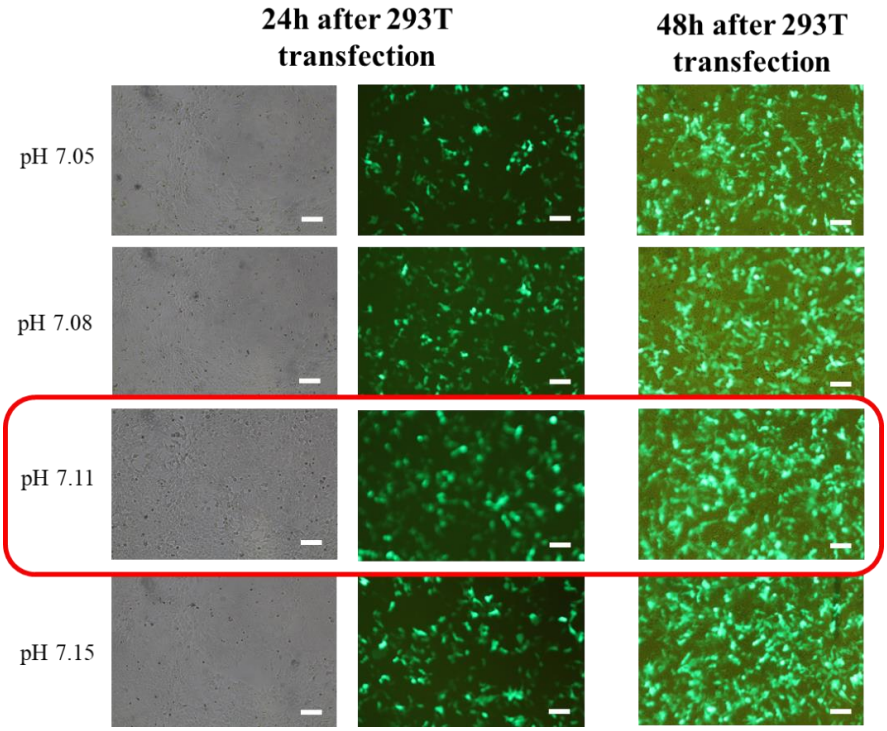

Figure S3 – Ideal 2x HBS buffer for HEK 293T transfection. Four T25 HEK 293T cells were transfected with GFP plasmid and different pH of 2x HBS buffer (pH 7.05; pH 7.08; pH 7.11 and pH 7.15) were tested to identify the most efficient for Calcium-phosphate transfection protocol. Approximately 24h and 48h after transfection, the cells were visualized in a fluorescence microscope. The red square indicate the chosen pH from 2x HBS buffer chosen to further transfections using the lentiviral transfection protocol. Scale bar = 100 µm

A.

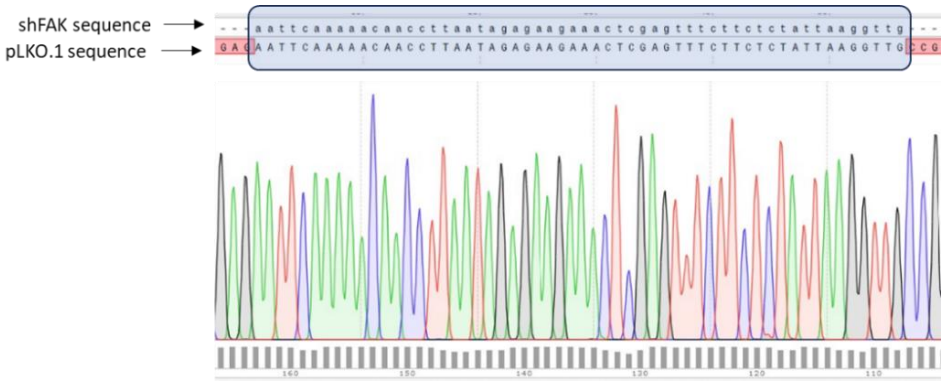

B.

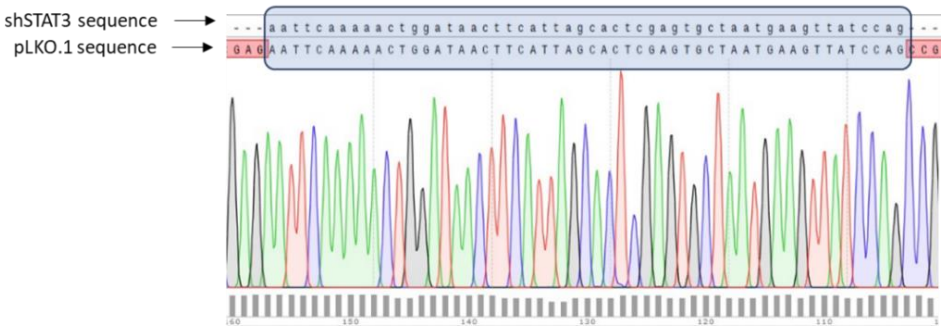

C.

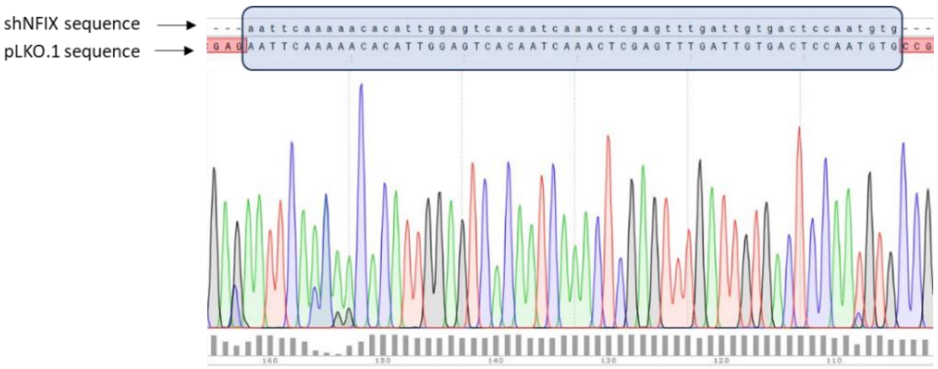

Figure S4 – shRNA cloning into pLKO.1 plasmid. Sanger sequence alignment of shRNA FAK (**A.**), STAT3 (**B.**), and shRNA NFIX (**C.**) oligo sequenced and the cloned pLKO.1 construct. Sequencing was performed with U6 primer (see table S2 in annex). The black square indicates the perfect match of the target shRNA sequence insertion into pLKO.1 plasmid. The red squares indicate no sequence match. The alignments and the analysis of the Sanger data were performed using the SnapGene software.